TPK
Solar Systems Inc.

(Now TPK International Inc.)

Final Report

DEVELOPMENT OF A PHOTOVOLTAIC POWERED REVERSE OSMOSIS WATER DESALINATION SYSTEM

(DSS File No.: 51Sz.23216-5-7272)

T3-W5
85-7272

36 Bentley Ave., Nepean, Ontario, Canada K2E 6T8 Tel. (613) 225-4403 Telex: 053-3930

SUMMARY

TITLE: DEVELOPMENT OF A PHOTOVOLTAIC POWERED REVERSE OSMOSIS WATER DESALINATION SYSTEM

CONTRACTOR:
TPK International Inc.
36 Bentley Ave. Nepean, Ont.
K2E 6T8 (613) 225-4403

CONTRACT No.:
1SZ85-00188
DSS File #
51SZ.23216-5-7272

DURATION: 22 months
(Feb. 1986 - Dec. 1987)

COST: $35,647.00
Fiscal Years
1986/87 & 1987/88

OBJECTIVES:

To develop a photovoltaic-powered reverse-osmosis system for desalination of brackish water. To test the system to characterize its operation and to evaluate its performance in the laboratory.

RESULTS:

The laboratory prototype system operates from a 24 V battery which is charged by a 740 watt PV array. The RO system operates at 1.4 MPa and produces about 3 Lpm of water with 98 % of the salt removed, at an energy cost of 10 kJ/L. The system worked well during a ten day trial under automatic control.

CONCLUSION:

The system functions as designed, economically providing about 1000 L/day of drinking water. Further development is required before the system will be ready for marketing.

RECOMMENDATION:

That development continue, to produce a PV/RO system for use in real-world applications and that such a system be subjected to Canadian field trials.

FINAL REPORT

DEVELOPMENT OF A PHOTOVOLTAIC POWERED REVERSE OSMOSIS WATER DESALINATION SYSTEM

RENEWABLE ENERGY DIVISION

PREPARED FOR:

Renewable Energy Division
Coal and Alternative Energy Branch
Energy, Mines and Resources Canada
Ottawa, Canada
DSS Contract File No.: 51SZ.23216-5-7272

December, 1987

PREPARED BY:

C.E. Norman
TPK International Inc.
36 Bentley Ave.
Nepean, Ontario
K2E 6T8
Phone: (613) 225-4403

SCIENTIFIC AUTHORITY:

Mr. J. Larry McClung
Technology Coordinator, Photovoltaics
Solar Energy Development Program
Renewable Energy Division
Energy, Mines and Resources Canada

RESTRICTIONS ON DISCLOSURE

The design concepts, prototypes, test techniques and results described in this report are confidential. As such, they shall not be disclosed outside Energy, Mines and Resources Canada or be duplicated in whole or in part without the express, written consent of an authorized officer of TPK International Inc., for a period of 12 months. This restriction does not limit the Crown's right to use information contained in the report if it is obtained from another source.

TABLE OF CONTENTS

	Acknowledgments	i
	Preface	ii
	Abstract	iii
	Executive Summary	iv
1.0	INTRODUCTION	1
2.0	REVERSE OSMOSIS MEMBRANES AND SYSTEMS	4
3.0	POWER CONDITIONING AND CONTROL OPTIONS	8
4.0	PROTOTYPE PV/RO SYSTEM DESIGN	13
	4.1 Component Selection	13
	4.2 Expected Operation	16
5.0	POWER REGULATOR AND SYSTEM CONTROL ELECTRONICS	18
	5.1 System Control Circuitry	18
	5.2 Modified Voltage Regulator	19
	5.3 Construction and Testing	21
6.0	COMPONENT TESTING AND SYSTEM INTEGRATION	23
	6.1 System Assembly and Integration	23
	6.2 Motor Testing	24
	6.3 Piston Pump Testing	25
	6.4 Design Modifications and Retesting	27
	6.5 RO Element Test Results	28
	6.6 Expected System Performance	29

..../cont'd

7.0 SYSTEM TESTING 31
7.1 System Monitoring 31
7.2 System Functional Tests 32
7.3 Steady State Operation 34
7.4 Transient Operation 37
7.5 Long Term Automatic Operation 40

8.0 EVALUATION AND DISCUSSION 44
8.1 Evaluation of Prototype System 44
8.2 System Redesign 46

9.0 CONCLUSIONS AND RECOMMENDATIONS 49

REFERENCES 51

APPENDICES
Appendix A 52
List of Figures and Tables 53
Figures and Tables 55

ACKNOWLEDGEMENTS

The author would like to acknowledge the contributions of Olie Kutowy of the National Research Council of Canada, Division of Chemistry, for his assistance in introducing reverse osmosis concepts, for his valuable suggestions and for inspecting the prototype PV/RO system and test methods at TPK International Inc. In addition, the author wishes to thank those at TPK who helped make this project a success: Albino Genovesse, Gianfranco Petrilli and Gordon MacKenzie for their technical assistance; and Dr. Raye Thomas and Jenny Hull for their administrative help.

Funding for this project was provided by the Panel of Energy Research and Development, Office of Energy Research and Development, Energy, Mines and Resources Canada.

Norman, C.E., TPK International Inc. Development of a Photovoltaic Powered Reverse Osmosis Water Desalination System. Report of Contract File # 51SZ.23216-5-7272. Renewable Energy Division; Energy, Mines and Resources Canada, Ottawa, Ontario. 1987. (88 pp.)

Copies of this report may be obtained through:

Renewable Energy Division
Energy, Mines and Resources
580 Booth Street
Ottawa, Ontario
K1A 0E4 CANADA
(613) 995-1118

OR

Interlibrary Loans
CISTI Library
National Research Council
Bldg. M-55, Montreal Rd.
Ottawa, Ontario
K1A 0S2 CANADA
(613) 993-1585

This report is distributed for informational purposes only and does not necessarily reflect the views of the Government of Canada nor constitute an endorsement of any commercial product or person. Neither Canada, nor its ministers, officers, employees or agents makes any warranty in respect of this report or assumes any liability arising out of this report.

PREFACE

This report describes the engineering development and testing of a desalination system for brackish water, powered by solar electric (photovoltaic) modules. The system is intended for use in remote areas where potable water and electric power are not now available. The primary application is expected to be the supply of drinking water for village or livestock use in developing countries or remote parts of Canada. In its present form, the system can provide about 1000 litres per day of drinking water, at a cost of less than one cent per litre. The design is flexible and can easily be adapted to larger or smaller sizes. The system consists of a 24 V battery, DC motor, high pressure pump, reverse osmosis membranes, a filter and an electronic controller, and is powered by an array of 24 standard PV modules.

The report deals mostly with the technical details of the system design and testing and is primarily intended for people interested in small-scale applications of photovoltaic power. The report and the PV/RO system itself will, however, also be of interest to anyone involved in water supply and treatment for developing countries or remote areas in Canada. While the report is not highly technical, the reader is assumed to have some knowledge of solar energy, photovoltaics, electronics and general science.

The report is quite specific, describing the development of a particular system. Although the concepts of reverse osmosis are introduced, the report is not intended as a general treatment of the subject, nor as an introduction to photovoltaics. Neither is it a user manual or instruction guide for the prototype system. The system described is a laboratory prototype and not designed for any field application. Its design is expected to change considerably as development continues towards a marketable product. Finally, the technology described is proprietary to TPK International and the Crown, and therefore may not be used by any individual or organization in any way which would jeopardize the interests of the owners.

ABSTRACT

Reverse osmosis is an efficient method for desalinating brackish water. In remote areas, photovoltaic modules can provide dependable, cost-effective power. A small, PV powered RO system can therefore be used to provide potable water from brackish water in remote regions. This report describes the development and testing of such a system, designed to provide 1000 litres per day of drinking water.

The prototype PV/RO system is based on three thin-film RO elements in series pressurized by a small, positive displacement pump which in turn is driven by a permanent magnet DC motor from a 24 V battery. The 740 W_p PV array charges the battery through a modified voltage regulator. The system is controlled electronically. The incoming feed water is filtered, while the system pressure is controlled by a regulator valve at the brine discharge. Further work is required to develop the system for field use.

The prototype system was tested under transient and steady state conditions over a wide range of operating pressures and temperatures, and with feedwater salinities of 1000 to 5000 ppm of NaCl. The system performed as expected. The optimum operating pressure was found to be about 1.4 MPa, at which 38 % of the feed water was recovered as product water at a flow of 3 Lpm and 98 % salt rejection. The energy cost of this water was found to be about 10 kJ/L. On a typical day with 18 MJ/m^2 insolation, the system will produce the targeted 1000 litres of drinking water. After testing, the system was operated automatically and monitored during a ten day trial period.

EXECUTIVE SUMMARY

In many areas of the world, there is no fresh drinking water, but brackish water, containing 1000 to 5000 ppm by weight of dissolved salts, is available. In these cases, reverse osmosis can be used to desalinate this water to make it potable. In the reverse osmosis (RO) process, water is forced, at high pressure, through a semi-permeable membrane, leaving the salts behind in a concentrated brine. The resulting permeate is relatively salt free. In many of these same areas, grid power is not available to power the system. In such cases, photovoltaic (PV) modules can provide dependable and economical power. The combination of PV power with reverse osmosis is therefore a cost-effective approach for remote water desalination.

This project involved the development and testing of a prototype PV/RO desalination system. The system was designed to produce 1000 litres of potable water during a day having 18 MJ/m^2 of insolation. The purpose of the project was to investigate the combination of PV power with RO desalination and to design the system for most efficient use of the available solar energy.

The design is based on three, commercially-available RO elements connected in series, each consisting of a spiral-wound thin-film membrane in a pressure vessel. The feed water is pumped through a particulate filter and into the RO elements. The brine is released through a pressure regulating valve which controls the system pressure. Depending on the operating

pressure, up to 40 % of the feed water can be recovered as permeate. Two types of high-pressure pump were tested. An inexpensive piston pump, though efficient enough was too noisy and proved unsuitable. A somewhat less-efficient, but smoother-running rotary positive displacement pump was then selected. Initially, a second, small, feedwater pressurizing pump was selected to push the water through the filter. However, it proved to be incompatible with the main pump and unnecessary in a laboratory system and was therefore not used.

The main pump is driven by a permanent-magnet DC motor powered by a 24 V lead-acid battery. The battery is kept charged by an array of 24 PV modules which provide up to 740 watts at a peak current around 25 A. The battery charging is controlled by a modified TPK voltage regulator. An alternative power control approach was considered, consisting of a maximum power tracker to provide a continuous impedance match between the PV array and the motor which would thereby operate at a variable speed. After some analysis, this approach was discarded as being more costly and complex, yet less efficient than the battery based system.

An electronic controller was designed to automatically operate the system. Its primary function involves turning on the motor to start up the system when the battery charges above a preset voltage, and shutting off the system when it discharges below a second, lower voltage. In this way, the system adjusts itself to the amount of sunlight available, without excessive turning on and off or deep cycling of the battery. The controller also monitors the system pressure and

shuts down the system if it is too high or low. Due to pressure pulses and a logic error, however, the circuit caused numerous false shutdowns. These safety functions were therefore disabled for long term testing. Finally, the circuit monitors the permeate conductivity and actuates a solenoid to reject the permeate if it is too salty; ie. during the first two minutes after startup.

The major components of the system were tested to determine their characteristics and compare them with the manufacturers' specifications. On the basis of these results, the expected performance of the system was calculated. The completed system was then tested in steady state operation under a wide range of pressure and feedwater conditions. The test solution consisted of NaCl dissolved in deionized water. This solution was prepared to a known concentration and recycled by mixing the brine and permeate back into the feed water. A calibrated conductivity cell was used to determine the permeate salinity. During testing, the battery voltage, motor current, system pressure, brine and permeate flows were all measured. The results were analysed to determine the specific energy per litre of permeate, the pump/motor efficiency, the salt rejection and the permeate recovery fraction. The transient operation at startup and shutdown was also recorded.

The system performed very much as expected, the permeate flow increasing with pressure and feedwater temperature, and decreasing for saltier feed water. The design pressure was found to coincide with the optimum operating point where the specific energy was minimized. This occured at a pressure of

1.4 MPa (~ 200 psi) and a permeate flow of ~ 3 Lpm, representing a recovery fraction of 38 %, close to the maximum allowed for the RO elements selected. The salt rejection in the permeate was over 98 % under these conditions. The motor efficiency was almost 80 % while that of the pump was around 50 %.

After characterizing the system, it was allowed to operate under automatic control for a period of ten days. A data logger and manual spot checks served to monitor the system performance during this period. The solar irradiance, battery voltage, source and load currents, and RO system parameters were all recorded and analysed to determine the daily energy usage and product water volume. The results indicated that the specific energy is less than 10 kJ/L of permeate, and that the system will provide more than the required 1000 L/day of drinking water.

The system is a laboratory prototype at present, and much development work remains to be done before it can be placed in the field in a real-world application. Several improvements can be made to the basic RO system, and the controller should be redesigned to correct its false shutdown problems. For field use, the component mounting and connections will have to be improved. In addition, feedwater pretreatment and/or membrane backwash features may be required in some applications. However, the project was quite successful in meeting its goals, and has served to prove the concept and advance the development of PV/RO desalination.

1. INTRODUCTION

There are many places in the world and even in Canada where fresh or potable water cannot be found, but where plentiful supplies of sea water or brackish water is readily available. To render this water fit for human consumption or livestock watering, it must be purified by removing the dissolved salts. The most efficient means of doing this is reverse osmosis, a process whereby a fraction of the water is forced under high pressure through a semi-permeable membrane [1]. The pores in the membrane are large enough to let the water molecules through, but too small for the larger ions and heavy molecular weight molecules. In essence, the "permeate" water is filtered on a molecular scale, leaving the dissolved salts in a concentrated brine which is then discarded. Reverse osmosis is now being used in many industries for a variety of concentrating, separating and purifying purposes [2]. The application considered here, however, is remote water desalination.

Many of the locations where desalination is required are also remote from conventional power sources. In most of these applications, photovoltaic (PV) modules can provide the necessary power reliably and at a relatively low cost compared to alternate power sources. The combination of photovoltaics and reverse osmosis (RO) therefore appears to be a good one for remote water purification.

For PV powered sea water desalination, Highquest Engineering and Seagold Industries (both in British Columbia) have developed a highly efficient RO system based on their

unique energy recovery pump [3]. In this piston pump, the waste brine, still at a high pressure, helps pump the sea water feed (which contains about 35,000 ppm of dissolved salts) by pressing on the back of the piston. In all other RO systems, the brine is simply released through a pressure valve and its hydraulic energy is lost. (TPK supplied the PV array and a microprocessor based system controller and maximum power tracker for the prototype energy recovery PV/RO system in 1984 [4].) Although the custom-made energy recovery pump is quite expensive at present, it appears to be the most cost effective approach to PV powered sea water desalination.

For desalination of brackish water (2000 to 5000 ppm total dissolved solids), however, the situation is quite different. The operating pressures are much lower for brackish water and the permeate recovery fraction is much higher. Thus, the energy lost in the release of the brine is not as significant in brackish water systems and therefore does not warrant the purchase of an expensive energy recovery pump. For these reasons, in this project, it was decided to focus on developing a system using commercially available components for brackish water desalination applications.

The purpose of this project was to develop a prototype photovoltaic powered reverse osmosis system for remote desalination of brackish water. The design specifications are given in Table I. The goal was to produce about 1000 litres of fresh water per day using a 750 Wp PV array with an insolation of 18 MJ/m^2/day on a horizontal surface. Since silica, organic matter and hardness in the feed water can complicate the RO

system design and operation, the prototype system was designed for a simple test solution of NaCl in filtered, deionized water.

This final report presents the work done on the design construction and testing of the prototype PV/RO system. The theory of reverse osmosis membranes and systems is introduced in Section 2. In Section 3, two power control options, namely maximum power tracking and storage battery, are presented and compared. The component by component design of the prototype system is described in Section 4. Design of the power regulator and control electronics are discussed in section 5. Section 6 deals with the testing of the individual components and integration of the overall system. In Section 7, the system test methods and results are presented and analysed. Evaluation and redesign of the prototype system are the topic of Section 8. Finally, Section 9 presents the conclusions and recommendations for the project.

2. REVERSE OSMOSIS MEMBRANES AND SYSTEMS

The heart of any RO system is a semi permeable membrane with pores on the order of 1 nm in diameter. The membrane itself is very thin but is bonded to and supported by a thicker fabric. Usually, a back-to-back double membrane layer is edge sealed and rolled up to make a spiral-wound RO element. The feedwater enters at one end of the roll and the concentrate or brine exits at the other end after passing over the entire membrane surface. Under pressure, some of the feedwater is forced through the membrane. This permeate or product water percolates along the fabric, around the spiral and is collected at a central tube. The entire element is wrapped in fibreglass and placed inside a pressure vessel or cartridge. A typical spiral-wound element is 4" in diameter and 40" long. Typical elements are designed for tap water, brackish water or sea water applications. *.

Until a few years ago, the only readily available membranes were made of cellulose acetate. Recently however, thin film composite membranes have been developed. While they are more expensive, they have better properties [5]. They operate at substantially lower pressures and still achieve higher salt rejection. Thus, they are more efficient on the basis of energy used per litre of permeate. They are also more resistant to pH extremes and less susceptible to bacteriological decay than the cellulose acetate membranes. Their chief drawback is that they cannot tolerate free chlorine in the water. Thus, chlorine disinfectants cannot be used to pretreat the water. This is not generally a problem however,

* Introduction to RO membranes courtesy of O. Kutowy and A. Tweddle of the National Research Council.

since natural water sources do not contain free chlorine.

Some specifications for a typical thin film RO element (from Filmtec Corp., a manufacturer of RO membranes) are included in the Appendix. Steady state operating characteristics for this element are illustrated in Figure 1 in which the feed water pressure versus permeate flow is plotted. The typical salt rejection percentage is also shown. The intercept on the pressure axis represents the osmotic pressure between the feed water and the permeate. At low flow rates, the operating pressure is low, but so is the permeate flow, and salt diffuses through the membrane reducing permeate quality. Higher pressure is required to push more water through the membrane. A sea-water membrane is thicker than a brackish water membrane for higher salt rejection but it also requires a much higher operating pressure.

If the feed water flow is too low, salt polarization at the membrane can limit the permeate flow. Also, each element has a maximum recovery fraction, Fr - the ratio of permeate flow to feed water flow - which depends on the silt content and hardness of the water. If the feed water flow is too low, not only will there be polarization effects, but the membrane will clog up with silt and require more frequent cleaning. The maximum recovery fraction and other operating parameters are given in the specifications for the particular element (see appendix).

Two RO system configurations are depicted in Figure 2. Both can be designed to operate at the same net flows and pressures. In the first, there are multiple, small,

series-connected elements. The slighty concentrated brine from the first serves as the feed water for the second (Qf_2). The permeates combine as the product water. In this way, the net recovery fraction can be greater than that allowed for a single element - up to 50% in some applications. The system is driven by a high pressure pump; often a rotary positive displacement pump for small systems. A standard AC motor turns the pump at a fixed speed and the system pressure is controlled by an adjustable release valve at the brine discharge. Water is supplied by a feedwater pump and passed through a particulate filter to protect the main pump from grit and to keep any silt out of the RO elements. Often, there are pressure switches and other electrical devices to control the system.

The second system in Figure 2 uses a single, larger RO element and a third, recirculating pump to provide the same net permeate flow. Most of the brine is recirculated (Qr) to maintain a high flow (Qf) across the membrane surface to allow a high permeate flow (Qp) without exceeding the maximum allowed recovery. The recirculation pump provides a small pressure boost (a few psi or kPa) to keep the water flowing and thus does not require much drive power. It must, however, withstand the high system pressure (typically 300 psi or 2 MPa). The rest of the system is identical to the previous one.

This second approach is probably less expensive than the first since only one element (and pressure vessel) is required. However, it is difficult to find an efficient, high-system-pressure recirculating pump for small systems. Also, some energy is wasted just pumping the high flow around

the loop. Finally, the system is more difficult to design and operate, having an extra degree of freedom. For these reasons, it was decided to avoid the use of a recirculating pump and design the prototype PV/RO system using multiple elements.

Conventional small RO systems are designed for minimum capital cost, 24 hour per day operation and ease of use. Little consideration is given to energy efficiency since AC power is used. In a photovoltaic powered RO system, however, the power supply usually represents the major capital investment so that efficiency becomes very important. This affects the type of pump, the membrane operating pressure and optimum recovery fraction. In addition, the system must run intermittently and from a variable DC power source. Thus, the design of such a system is quite different. The basis for evaluating PV/RO systems should be cost per volume of permeate over the life of the system. This is closely linked to the energy required per unit volume (kWh/m^3 or joules per litre).

3. POWER CONDITIONING AND CONTROL OPTIONS

There are two basic approaches to running an intermittent load from a variable and power limited source such as a PV array. The first is to isolate the load from the source by means of an electrochemical storage battery between the two. In the second, a maximum power tracker is used to instantaneously match the power available at the source to the load. Power conversion block diagrams and the salient operating features of the two approaches are outlined in Figures 3 and 4.

The battery powered system (Figure 3) is the simpler of the two, both to design and to understand. The array converts solar energy into electricity which is stored chemically in the battery. When the RO system operates, the battery drives the motor which converts the power to mechanical rotation. The pump then converts it to hydraulic power (pressure x flow) which in turn drives the reverse osmosis process. Each step in the chain can be characterised by a power conversion efficiency. The operating point is almost constant, being defined by the battery voltage and the brine release pressure setting. The feed water pump and any system controls act as secondary loads on the same battery. The modified voltage regulator provides the primary system control functions: keeping the battery from overcharging, and automatically turning on and off the RO system.

Under normal operating conditions, the system will be off in the morning when the sun rises (Figure 3). As the PV array output current increases, the battery begins to charge. At some point, the battery voltage rises to the turn-on threshold (the

"load reconnect" voltage of the modified regulator), and the system starts up, drawing a constant current during its operating period. If the array current is higher than the load current, the battery will continue to charge. If less, the battery will begin to discharge, providing the remaining current to the load. Thus, the system gives a constant product water flow even during cloudy periods. Once the sun sets, power to the load is provided entirely by the battery which will slowly discharge down to its modified "load disconnect" voltage, at which point the system will shut down for the night. The state of charge of the battery changes throughout the day as shown in Figure 3. Clearly, the on and off threshold voltages must be carefully set to avoid fully charging the battery, but to keep the average state of charge high. For maximum battery utilization, the daily depth of discharge should be about 25 to 35 %. Note that during much of the day, the load operates directly from the array with the battery acting to regulate the voltage. Thus, there is minimal energy lost due to battery inefficiency.

Most of the maximum power tracker (MPT) based system (Figure 4) is the same. The MPT however, replaces the regulator and battery. The MPT acts like a DC to DC transformer with a variable "turns ratio" to keep the array operating at its maximum power point and thereby maximizing the power to the load on a moment by moment basis [6]. The MPT is characterised by a tracking efficiency (power to load / maximum power available from the array) which varies with the operating point but is typically about 90 % [6]. There is no long term energy

storage and so the system operating point changes with the sunlight level. The system will only operate above some threshold level of irradiance and below that level it is turned off. At higher levels, the permeate flow increases, reaching a maximum under peak sunshine.

Unlike the battery based system, the MPT system cannot operate at a constant pressure as set by a brine release valve. To do so would unnecessarily constrain the operating range or force the system to operate at an inefficiently low recovery fraction most of the time (see discussion below). The best alternative (short of an automatic feedback controlled adjustable regulator) is a simple needle valve or orifice for which the pressure would be proportional to the square of the brine flow.

The RO system operation can be understood better with the help of Figure 5 which plots the relationships between the operating parameters of the RO elements. This particular plot is for the system designed in Section 4 and is based on three series-connected Filmtec TW30-2540 RO elements. These operate as would a single 2.5" diameter element 120" long. Figure 5 includes feed water flow (Qf) and system pressure as the two independent variables for a fixed feedwater salt concentration. The oblique lines meeting at the osmotic pressure intercept represent lines of constant recovery fraction, Fr. The permeate flow is not plotted but is simply the product of Fr and Qf. The curves are lines of constant hydraulic power:

Phyd = pressure x Qf x density x acceleration of gravity.

Under normal conditions, the system must operate within

the triangle bounded by the three dashed lines. At the top is the maximum allowable feed water flow (see specifications in appendix). To the left of the vertical line, the salt rejection is less than 90 % and the permeate quality is unacceptable. The slanted dashed line represents the maximum allowable recovery for three series elements with low silt feedwater. At higher recovery fractions, the system will operate but only until the membranes clog up.

The most energy efficient operating point is at the lower apex of the triangle, representing low pressure, minimal quality and maximum recovery. At this point however, the permeate flow is low and its quality will never be good. The specified operating point from Table I is also indicated in Figure 5. The range of operating points for an MPT system is shown as the curved line ending at the right corner of the triangle. It was calculated on the basis of the pressure vs flow relationships noted in Figure 4. To make best use of the MPT system, the curve was adjusted so that its top end corresponds to peak sunlight on the array. In contrast, the operating point of a battery based system can be adjusted to lie anywhere in the triangle simply by adjusting the brine regulator pressure and the pump speed (assuming a speed-reducing transmission is available). The actual operating point will wander around slightly as the voltage and temperature changes.

The two power-conditioning options are compared in Table II. Clearly, the battery based system is preferable. The design and controls are simple and very flexible. More modules and

batteries can readily be added to extend the daily operating period. On the other hand, the design of a maximum power tracker and any peripheral controls is anything but simple [4,6]. The battery system has inherent backup capacity for emergencies or cloudy days. It is true that batteries weigh more and have a limited life, but these drawbacks are minor in most applications. Most important is that the battery system costs less while producing more product water per day than does the MPT based system. Two reasons for this are the sub-threshold energy lost in the MPT system and the fact that the battery system can be adjusted to operate at a single efficient point while the MPT system operates over a wide range of points, only a few of which are efficient.

For these reasons, it was decided to design the prototype PV/RO system based on battery storage. This simplifies the design, construction and testing and should result in a more reliable, cost effective system.

4. PROTOTYPE PV/RO SYSTEM DESIGN

4.1 Component Selection

The prototype system was designed on the basis of the foregoing discussion and the specifications given in Table I. A block diagram of the system is shown in Figure 6. In selecting the components, only readily available stock items were considered. Cost and efficiency were other important factors.

The design begins with the selection of the RO elements. Filmtec has a wide selection of thin film composite membranes for use with sea, brackish or tap water. The tap water elements have the same specifications as the brackish water ones except for a lower maximum pressure rating. The cost is also lower. The elements come in three diameters up to 8" and in three lengths up to 40" long. The TW30-2540 element (see Appendix) was selected to fit the feedwater flow specification. Three series elements are used to raise the net recovery fraction from the 15% maximum per element to a total of about 42%. Pressure vessels for the three elements were also ordered.

The next major component is the system pressurizing pump. Many types of pumps are available [7], but for low-flow, high-pressure applications, a positive displacement pump is superior to a centrifugal type. Up to about 150 psi (1 MPa), a rotary vane or gear pump with an efficiency of 40 to 50 % is the best choice, while a piston pump is usually more efficient at higher pressures. Since this system is expected to operate around 200 psi, a piston pump was selected. Several manufacturers have suitable units. The pump casing, valves and piston should be compatible with salty water (ie. bronze or

stainless steel), and the pump should be able to run directly off the motor shaft at a high speed (eg. 1800 rpm). A Hypro model 5320BHR unit was selected. It develops a flow of 8.5 lpm at a pressure of 200 psi with an efficiency around 60% when driven at 1800 rpm. Some piston pumps are more efficient (~80%) but run at lower speeds (~400 rpm) and therefore are larger, more expensive and require a transmission.

The feed water to the system should be prefiltered to protect the piston pump from abrasive grit and the RO membranes from silt. A standard cartridge filter is used for this purpose. While not essential for a laboratory system, a feedwater pump would usually be required to deliver the water to the piston pump inlet. Any small pump with the right flow, driven by a 24 VDC motor would be suitable. A Flojet model 2000-132 double acting diaphragm pump was selected. It is self priming, easy to use and reasonably efficient. Since any piston pump produces a pulsating flow, the system has a simple standpipe to absorb the flow peaks and filter out the pressure pulses. This and the other pressure plumbing are made of hard copper pipe, joined with high temperature solder, suitable for use up to 300 psi. The final hydraulic component is the brine release valve which is adjustable to control the system pressure and thereby, the permeate flow.

The piston pump is driven by a 24 VDC permanent magnet brush type motor procured from Pacific Scientific (model No. BA 3628-7012-9-48B). The brush type PM DC motor is the most reliable and efficient for applications under 2 HP [7] and 1800 rpm is the most common speed rating for these motors. In

principle, any operating voltage can be selected, but for a battery based system, 24 V is an appropriate value. For trouble-free operation, sealed, maintenance-free, starved-electrolyte batteries from Power Battery Corp. are being used. Four PRC-6165 six-volt batteries are connected in series to achieve 165 AH capacity at 24 V.

The system power controller is a modified TPK VR-24S voltage regulator. It provides overcharge protection and has a load disconnect relay with adjustable voltage switch points. The load disconnect and load reconnect voltages are adjusted to maintain the battery state of charge within a range as discussed in Section 3. This regulator does not need the temperature compensation or trickle charge options but has oversized power relays to handle the high array and motor currents. The regulator is described further in Section 5.

The prototype system will be powered by a 740 Wp photovoltaic array. The array consisted of 24 TPK SW3404 PV modules, each producing 31 watts under peak operating conditions. The modules were connected 2 in series by 12 in parallel to charge the 24 V battery at a maximum current of about 25 A. The modules are mounted on a portable array structure with an adjustable tilt angle for easy setup and operation [8].

The remainder of the system consists of the control circuitry and its associated sensors and actuators as shown in Figure 6. The feedwater and system pressure transducers, P1 and P2 indicate whether the system is operating normally. If P1 is too low, the prefilter may be clogged. If P2 is low, it may

signal a ruptured membrane, while a high P2 indicates a plugged brine release valve. Any of these conditions should cause a system shutdown to prevent damage. The flow meter shown in Figure 6 is for research purposes only. Both pressure transducers and the flowmeter were purchased from Omega Engineering. The conductivity cell monitors the permeate quality. It consists of two stainless steel electrodes immersed in the permeate stream. If the conductivity is high, the permeate is too salty and is rejected either to the drain or back to the feed water inlet via the bypass solenoid. The control circuitry to perform all these functions is described below in Section 5.

4.2 Expected Operation

Each of the major components in the above power train has been sized and selected to match the others. Calculation of the system performance begins with the expected operating point of the three RO elements. From Figure 5, and the Hypro pump specification, the expected feedwater flow is 8.5 Lpm. At a maximum recovery of 42 % (and resulting permeate flow of 3.58 Lpm), the system pressure is 1.4 MPa (203 psi). Thus, the hydraulic power produced by the pump will be 199 watts. At 1800 rpm and 200 psi, the pump efficiency should be about 60 % so that the mechanical shaft power required is 332 watts. Thus, a 1/2 HP motor can be used. From the motor specifications, its efficiency should be around 78 % so that the electrical power required is 426 watts. At 24 volts, this represents a load of 17.8 A. The Flojet pump and control electronics are expected to

add another 1.3 A, giving a total load of 19.1 A for the system in steady state operation.

These energy transfer calculations are extended to derive the daily product water flow. If the battery voltage is 24 VDC, the array voltage, with blocking diode and resistance losses, will be 26 to 27 V. At a NOCT (normal operating cell temperature) of 50 °C, the 740 Wp array will provide about 660 W under peak sunlight at a maximum power point of about 28 V. Thus the peak charging current at 26.5 V will be about 24.5 A. With an insolation of 18 MJ/m²/day, equivalent to 5.0 hours of peak sun, the array should generate 122.5 AH/day of charging. About half the time, the array drives the motor directly so there is no energy lost in the battery. During the remaining time, the battery AH efficiency will be about 95 % so that about 119 AH/day will be available to the load. Hence, the load should run for 6.25 hours per day at 19.1 A, giving a total permeate volume of 1343 litres per day. The electrical energy cost of this water is determined (by combining the above results) to be about 2.1 kWh/m³ or 7.7 kJ/L.

5. POWER REGULATOR AND SYSTEM CONTROL ELECTRONICS

5.1 System Control Circuitry

The system controller monitors the system pressures and shuts the pump off under abnormal conditions. It also monitors the permeate water, rejecting it if the conductivity (salt content) is too high. The circuitry to perform these functions is depicted schematically in Figure 7.

Power from the battery is regulated down to 12 V and 5 V for the circuit supplies. The circuit inputs are monitored by comparators with adjustable thresholds. The two pressure transducers produce DC voltage levels between 1 and 6 volts, proportional to the pressure. If the feedwater pressure drops below the threshold, the output of 324A will go high, clocking the 4013A flip flop output high. This will turn on the transistor and LED to indicate a low feedwater pressure.

The system pressure transducer signal is handled in the same way through 324B and 4013B, turning on the output transistor and LED if the system pressure is too low. If the pressure is too high, comparator 324C will go high, clocking the second 4013A and turning on its output inverter/buffer transistor and LED. These three outputs (normally high) are wired together through diodes in a simple AND gate which is connected to the load disconnect relay in the voltage regulator. Thus, if any of the three pressure signals is abnormal, the system will shut down. To allow the system to start up when the pressure is low, the two low-pressure alarms are disabled via the reset lines of the 4013's during start up. The 555 timer provides a ten second reset pulse whenever the

pump is turned on at the voltage regulator.

The conductivity cell provides the last signal. Residual salt in the permeate water provides a current path between the two electrodes of the cell. Thus, the cell's output voltage increases non-linearly with salt concentration and permeate temperature [9]. When this signal rises above a preset threshold, the output of 324D goes high, turning on the darlington transistor pair and LED indicator. The transistor drives the bypass solenoid to reject the permeate until its conductivity drops to an acceptable value. The solenoid is only energised when the permeate is too salty. This normally occurs only during system startup after salt has diffused through the RO membranes and has to be flushed from the system. Finally, a manual reset button is provided to clear the flip flops and LED indicators after correcting a fault and before restarting the RO system.

5.2 Modified Voltage Regulator

The system batteries are charged using a modified TPK VR-24S voltage regulator. This proprietary circuit contains a low voltage load disconnect (LVD) relay and control circuit to protect the battery from complete discharge. In this application, the RO pump is always turned on and off via this relay. The system automatically turns on the load when the batteries are recharging and turns it off again when they are partially discharged. Several changes are therefore required in the LVD control circuitry to incorporate these features. The modifications are shown in schematic form in Figure 8.

First, the RO system will be off more often than on. Thus, to save energy and ensure that the pump is disconnected when power is turned off, the normally-open contacts of the load disconnect relay are used rather than the usual normally-closed contacts. Thus, the low voltage disconnect signal from the VR-24S control circuit must be inverted. This is achieved with the transistor added between the output of the 124B amplifier and the gate of the FET which drives the relay coil. In addition, the low voltage disconnect threshold should be higher than normal and adjustable so that the batteries will operate above 50 % capacity rather than mostly discharged. Finally, the voltage for reconnecting the load (ie. starting the pump when the battery is recharging) should be closer to the voltage at which it is disconnected to ensure that the daily battery discharge cycle is not too large a fraction of the battery capacity. For these reasons, the input and feedback resistors for the 124B amplifier have been changed and a potentiometer added to allow adjustment of the thresholds for normal on/off cycling.

The system shutdown signal from the monitor and control circuitry (Figure 7) is applied directly to the gate of the FET, allowing it to be turned off (and the pump to disconnect when the relay de-energizes) whenever a faulty pressure condition is detected. Normally in the VR-24S, the FET drain connects directly to the relay coil. In Figure 8, a manual override switch has been added. This allows the RO system to be turned on or off independently of the controller or VR-24S logic. Care must be taken when using this, however, to avoid

running the system under fault conditions or completely draining the batteries. Finally, the lower end of the relay coil provides the startup signal to the fault disable timer in the control circuit.

5.3 Construction and Testing

The modified VR-24S circuit was assembled on a standard VR-12S printed circuit board, with the appropriate changes made by cutting traces and adding components and wires. The normal 10 A charging relay was replaced with a 30 A relay to handle the 25 amperes expected from the PV array. Similarly, a larger Schottky rectifier was used for the blocking diode. Double strands of # 16 gauge wire were used to carry these high currents to and from the array, battery and load.

The control circuit was assembled on a perforated proto-board, with control wires soldered to the VR-24S board and wire-wrapped sockets for the IC's. The sensor and solenoid wires connect to the circuit via small, multipin plugs. The two circuit boards, power components, relays, terminals and manual switch are all mounted on an acrylic sheet. Photos of the completed controller are shown in figure 9.

The circuit was adjusted and tested by connecting a variable DC supply to the battery terminals of the regulator. The low voltage load disconnect threshold was adjusted to 23.7 volts, corresponding to a loaded battery with about 50 % remaining capacity. The corresponding reconnect threshold is 26.6 V which will not be reached until the battery is being recharged at a reasonable current. These two levels determine

the normal, automatic, daily cyclic of the system.

In automatic operation, the batteries should never reach a fully charged state since the pump would be turned on before that occured. To protect the batteries from overcharging, however, especially if the system is manually turned off, the VR-24S has an array disconnect relay and a trickle charge feature to properly float charge the batteries. The full charge termination threshold was adjusted to 29.3 V, suitable for the PRC 6165 batteries. The corresponding full charge resumption voltage was 24.5 V. This should ensure that the full PV array current is available to the load whenever the RO system is operating. The float voltage for the trickle charge mode was set to 28.0 V and the trickle charge current limit is 0.46 A.

The control logic was tested using potentiometers to simulate the pressure transducer and conductivity cell signals. The alarm thresholds were set to reasonable values for the three signals. During testing, all of the logic performed correctly, shutting off the load relay under appropriate conditions, and being disabled during start up. The circuit standby current (load off, array connected) is 39 mA and the load connect relay and array disconnect relay each have a coil current around 80 mA.

6. COMPONENT TESTING AND SYSTEM INTEGRATION

6.1 System Assembly and Integration

The assembled prototype RO system is shown in the top photograph in Figure 10. This can be compared with Figure 6. For convenience, the system was assembled on a plywood backplane. The photo is dominated by the three RO elements in their fibreglass pressure vessels. The motor and pump (the pump is quite small) are together on the shelf below the elements. The high pressure plumbing consists of hard-soldered copper pipe. The copper standpipe (to absorb flow pulses from the pump), pressure gauge and pressure transducer are on the right end, above the control electronics. The flow meter shown in Figure 1 was deleted since that flow is clearly the sum of the brine and permeate flows which both have to be measured anyway.

Feedwater comes in through the Flojet pump at the lower left of the photo. The filter housing appears above it. The waste brine and permeate both exit at the left end of the RO elements, the low pressure permeate through clear vinyl tubing to the conductivity cell and solenoid valve beside the feedwater pump. The brine exits through the adjustable relief valve which controls the system operating pressure. The four, six volt batteries are in cardboard boxes on the shelf below the rest of the system. The PV array, of course, is separate. It is mounted on a trailer support structure as shown in the lower photo in Figure 10.

The prototype RO system and photovoltaic array meet at the power controller. Integration of these three consisted of

providing them with power cables and making connections at the terminals of the voltage regulator. Large cables (AWG #6 or #8) were used to minimize voltage drops as DC currents up to 25 A occur. The conductivity cell, pressure transducer and permeate reject solenoid were also connected to the system control electronics using #22 gauge signal wire. The PV array was set up in an open parking lot behind TPK's plant. The 24 modules were wired two in series by twelve parallel to charge the 24 V battery. The array was positioned facing approximately south, with an inclination of about 45 degrees. The power cable to the controller is about 16 m long and has a manual switch to simplify disconnection.

6.2 Motor Testing

The 24 VDC permanent magnet motor was tested using a technique previously developed at TPK [7]. In this test, the motor shaft is coupled directly to the shaft of a second PM DC motor which is operated as a generator, driving a variable resistance load. The test motor is driven from a variable DC power supply. The motor and generator voltages, currents and shaft speed are measured over a wide range of steady state supply and load conditions. The results are then analysed to calculate the efficiency and torque of the motor at each operating point. This method is quick and inexpensive but accurate [7].

The results for the 24 V Pacific Scientific motor are presented in Figure 11. This graph depicts how the motor transforms power from voltage and current to speed and torque,

and indicates the efficiency of the power conversion. Lines of constant shaft speed and torque are plotted on the current vs voltage grid and the constant efficiency curves are superimposed. Thus, at 24 VDC and 20 A current, the motor should turn at about 1800 RPM and produce a torque of 2.0 Nm. This is the rated operating point for this motor. The efficiency at this point will be about 78.5 %, slightly higher than the rated value. The graph is plotted over a narrow range of voltages since the motor will operate from a nominal 24 VDC battery. The tests were done with the motor at operating temperature (typically 40 °C).

6.3 Piston Pump Testing

The Hypro piston pump was tested after installation in the system. The DC motor was driven from the battery at about 24 V and its voltage and current measured. The torque, speed and motor efficiency were then determined from Figure 11. The RO elements and pressure release valve provided a convenient hydraulic load for the tests. In fact, the elements were tested at the same time as discussed in Section 6.5. During these tests, deionized water was pumped through the system, with or without the feedwater pump. The "brine" and permeate were both returned to the feedwater tank. Before testing, the system was operated near its nominal operating point for several minutes to warm up the motor and flush out any air bubbles. During testing, a DC power supply was connected in parallel with the batteries to prevent them from discharging and reducing the voltage.

The test results for the Hypro pump are given in Table III. The controlled parameter for these tests was the system pressure as measured on the pressure gauge near the standpipe and controlled by the pressure relief valve setting. Motor current and voltage were measured with digital multimeters. The brine and permeate flows were measured separately by timing a known volume of the flow. Table III lists the measured and derived parameters for the pump. The electric power is the product of DC voltage and current. The motor speed and efficiency are found from Figure 11. The hydraulic power is the product of total flow, density and system pressure, adjusted to the correct units. The wire-to-water efficiency is the ratio of hydraulic to electric power. Dividing this by the motor efficiency yields the pump efficiency (ignoring any friction losses in the filter and plumbing). Finally, the ratio of permeate flow to total flow gives the recovery fraction for the RO elements.

The results given in Table III were further analysed to yield the flow vs pressure characteristics for the pump at a fixed shaft speed. This analysis was based on the fact that, as a positive displacement pump, the flow is directly proportional to the shaft speed. These results are plotted in Figure 12 which shows flow, pump efficiency and motor voltage at 1800 RPM as a function of pressure. The voltage is included only to relate the flow back to the motor and the rest of the RO system. The expected flow and efficiency (from the pump data sheets) in the anticipated range of operating pressures are also indicated. Clearly, the pump does not work as well as

expected. The flow is lower and drops off faster than expected with increasing pressure. The efficiency is also somewhat lower, at least at high pressures. The scatter among the data points indicates the degree of uncertainty or repeatability in the test results.

These disappointing test results are overshadowed by three other problems noted with this pump. When first operated, it was apparent that this is a very noisy pump. It has an unbalanced, reciprocating plunger and thus makes a lot of noise at 1800 RPM. Worse than this, it also vibrates a lot and thus causes the wooden back plane to vibrate via the rigid copper plumbing. Moreover, the pump did not operate stably. Its speed and flow would occasionally and suddenly change by a small amount, making precise measurements difficult. Finally, the fine print in the pump manual made it clear that this pump was not suitable for use with fluids intended for human consumption, presumably due to the seal materials and lubricants! For these reasons, the Hypro piston pump was removed from the system.

6.4 Design Modifications and Retesting

After some searching, a suitable replacement pump was found. It is a Procon rotary-vane, positive displacement pump. This is a simple, inexpensive, smooth running pump often used in RO systems. It is only rated for use up to 200 psi (~1.4 MPa), however, and unfortunately, is somewhat less efficient than even the Hypro pump. A brass bodied, model 2502 was selected for the correct flow at 1800 RPM. A special mounting

bracket was obtained to fasten the pump to the motor frame.

This pump was tested the in same way described above. It ran a lot quieter and smoother than the piston pump. The test results are listed in Table IV and the pump curves for 1800 RPM operation are given in Figure 13. Note that the flow and efficiency are close to their rated values, but that the efficiency peak is at a fairly low pressure. In the expected operating range (1.1 to 1.5 MPa), its efficiency is just below 50 %. At 250 psi (~1.7 MPa), the pump appears to be labouring heavily. This pump is therefore, not suitable for use much above 200 psi.

Another design change involved the feedwater pump. The Flojet pump used for this purpose is a diaphragm pump and thus produces a pulsating flow. Since it is in series, hydraulically with the main pump, there will be problems due to instantaneous differences in flow rate between the two. Indeed,even though the average flow from the Flojet was adequate, both the Hypro and the Procon pumps ran rough when fed by it. Apparently, the flow between pulses was not enough to maintain a positive feedwater pressure, thereby causing cavitation at the main pump inlet. When the Flojet pump was bypassed, the main pump ran smoother and more quietly, even though it then had to suck the water through the filter. Thus, for the prototype system, the feedwater pump was removed. This makes the system somewhat simpler and more efficient.

6.5 RO Element Test Results

The three series-connected reverse-osmosis elements from

Filmtec were tested as described above. From the results in Tables III and IV, the permeate flow vs system pressure can be plotted as shown in Figure 14. The results are for deionized water so that there is no osmotic pressure across the membranes. For the same reason, the salt rejection ratio could not be measured. The expected pressure range shown has been reduced by the value of osmotic pressure for brackish water. The permeate flows in this range are around the values specified for the system, but lower than expected from the Filmtec data sheets (see Figures 1 & 5). There is also some variation among the tests conducted on different days. Most of this difference and variability is likely due to changes in the water temperature (which was not measured in these tests). Water temperature is known to affect the permeability of RO membranes.

6.6. Expected System Performance

Based on the above test results for the pump, motor and RO elements, we can now recalculate the expected operating point for the integrated system. For maximum efficiency, the system should operate at the highest recovery fraction that the elements will allow. As discussed previously, this is about 42%. To derate for variations in water temperature and system voltage, however, the nominal recovery should be somewhat less - say 35 to 40 %. The recovery fraction increases with system pressure as shown in Table IV. By interpolating between test points, the pressure corresponding to a 38 % recovery is estimated to be about 1.1 MPa (160 psi). To this we must add

the osmotic pressure of the brackish water: about 0.3 MPa (44 psi), giving 1.4 MPa total (203 psi). This is the limit of pressure allowed for the Procon pump.

From Figure 13, at 1.4 MPa, the voltage is about 24.0 V which is the nominal battery voltage. Thus, the pump should turn at 1800 RPM and its efficiency should be 46 % and the total flow will be around 7.4 Lpm. The permeate flow at 1.1 MPa is 2.8 Lpm (from Figure 14), giving the 38 % recovery fraction. The hydraulic power at this pressure and flow is 170 watts and the motor efficiency (Figure 11) is about 79.5 %, giving an electric power of about 465 watts and a current of 19.4 A. The controller, while operating will draw another 0.1 A, for a total of 19.5 A.

The PV array has a peak charging current around 25 A. A typical day provides an insolation of 18 MJ/m2 on a horizontal surface; the equivalent of five hours of direct sunlight. The battery ampere-hour efficiency is typically above 96 %, and most of the time, the array current will go directly to the load, so that the effective efficiency will be even higher, say 98 %. Thus, during a typical day, some 25 A * 5 hours * 98 % = 122 AH is available to drive the RO system. At 19.5 A, it should therefore run on the average, about 6.3 hours per day. At 2.8 Lpm permeate flow, this corresponds to 1060 litres per day of product water. Of course, some of this may be rejected during start up, and the flow will doubtless vary due to voltage, temperature and salinity variations. The RO system would consume a total of 24 V * 19.4 A * 6.3 hr = 2.93 kWh (10.6 MJ) of energy, for a net energy cost of about 10 kilojoules per litre of product water.

7. SYSTEM TESTING

7.1 System Monitoring

To properly test the completed prototype system over a period of several days, it was necessary to monitor many of its parameters continuously and automatically. Figure 15 shows a simplified schematic of the monitoring sensors and circuitry used for this purpose. At the heart of the monitoring system are two 'Rustrak Ranger' data loggers. These are programmable, portable data acquisition units. Each can continuously monitor up to four signals of 0 - 2 VDC during a preselected logging period (up to several days). The data are stored as 12 bit words along with the time base. After logging, the data are played back through a serial cable to an IBM PC or compatible microcomputer for plotting or analysis using a software package that comes with the loggers.

As shown in Figure 15, five signals are monitored in this way. The solar irradiance is sensed by a reference cell with a low impedance load. This cell was calibrated against a standard Eppley pyranometer (courtesy of the National Research Council). The battery voltage is attenuated to reduce it to an appropriate signal level. Unfortunately, the loggers could not record differential or bipolar signals. Thus, only one signal from a current shunt could be monitored at any time and its negative side defines the signal ground for the other channels of that logger (logger 'X').

The second logger ('Y') monitors the signals from the system controller, referenced to its ground. The pressure transducer voltage and conductivity cell output are each

attenuated to a level suitable for the logger inputs. The pressure transducer was calibrated against the mechanical pressure gauge built into the RO system. The conductivity signal is non-linear with salt concentration and also varies with permeate temperature and, to some extent, flow. It is therefore used only as an indicator of permeate quality. The actual permeate conductivity is determined by sampling the permeate flow during steady-state operation and measuring the sample separately. A Beckman VSO1 RF-T-XT-4/12 conductivity cell was used for this purpose. This cell in turn was calibrated by testing precisely mixed solutions of NaCl in deionized water. In this way, the salinity of the permeate could be accurately measured.

The PV/RO system was not completely monitored by the sensors shown in Figure 15. The brine and permeate flows as well as the water temperature were measured manually. The water temperature is important since both the permeability of the RO membranes and the conductivity of a NaCl solution change with temperature. The flows were measured in steady state operation by timing a known volume of brine or permeate. In addition, the current signal from whichever shunt was not being monitored by the data loggers was measured manually with a digital voltmeter. The test setup and procedures were inspected by O. Kutowy from the National Research Council of Canada.

7.2 System Functional Tests

Once the complete system had been integrated, it was tested to ensure that it functioned as expected. The PV array

charged up the batteries correctly while the system was off during final wiring and calibration. A test solution of 3000 ppm (3 g/L) of NaCl in deionized water was prepared and pumped through the system to flush out previous water in the RO elements and plumbing. The solution was then recycled by mixing the brine and permeate back together in a large (~75 L) reservoir.

Initially, the system was operated manually at a pressure of 205 psi (1.41 MPa). The battery voltage was about 23.5 V and the motor drew about 18 A. The permeate flow was lower than expected: ~ 2.6 Lpm. This is probably because the water temperature was lower than during previous component testing. The permeate quality, however, was very good. The sample conductivity indicated a salt concentration of ~ 55 ppm, giving a salt rejection of 98 %. The water also tasted quite good!

The voltage regulator, system controller and data loggers were all tested and found to work correctly. In automatic operation, however, some problems were encountered with the control logic. High pressure glitches described below caused the system to shut down every 30 minutes or so. There is a more serious logic error in the control circuit itself. When the system shuts down normally due to low battery voltage, the pressure drops and the low-pressure alarm is set, preventing automatic startup the next day. To bypass these problems for testing purposes, the shutdown control wire from the logic circuit to the load disconnect circuit was cut. This still allowed the system to turn on and off automatically with changes in battery voltage.

7.3 Steady State Operation

The first set of tests was performed to characterize the system in steady state over a wide range of operating conditions. In an RO system there are three parameters which principally affect the product water flow and quality. These are the feedwater salinity and temperature, and the system operating pressure. Initially, the temperature and salinity were fixed and only the pressure varied to obtain some baseline operating data. The salinity was adjusted to 3000 ppm by weight, by mixing a weighed amount of water softener salt (iodide free NaCl) into a measured volume of deionized water. The feedwater temperature remained at 21 to 22 °C during these tests. The tests were then repeated at two other feedwater temperatures.

During the tests, the PV array was disconnected and the battery voltage remained between 24.0 and 24.5 V. At each operating point, the system pressure was adjusted by means of the brine discharge valve and the system allowed to stabilize before taking any readings. The system pressure, battery voltage, motor current, permeate flow, brine flow and feedwater temperature were then measured and recorded. The permeate and brine were also sampled to measure their conductivities.

Results of these tests are summarized in Figure 16. Here the permeate flow, salt rejection and specific energy are plotted as a function of system pressure for the three values of feedwater temperature parameter. Note that the salt rejection is one minus the ratio of product water to feed water

salt concentration, the latter being fixed at 3000 ppm. The specific permeate energy is the electrical energy required per litre of product water during steady state operation.

At a fixed temperature with a pressure just above the osmotic pressure, the permeate flow is low, the specific energy is high and the salt rejection is poor as the system is not operating efficiently. As the pressure rises, the permeate flow increases proportionally and the salt rejection improves as expected. The brine flow decreases as more of the feed water is forced through the membrane. Hence, the brine becomes more concentrated and the recovery fraction (ratio of permeate flow to feedwater flow) also increases. With a higher permeate flow, the specific energy drops and the system becomes more efficient.

As the pressure and permeate flow increase further, the recovery fraction eventually exceeds 40 % which is about the maximum allowed for long term use of the RO elements used in this particular system. At about the same pressure, the specific energy is minimized, starting to rise slightly at higher pressures. This broad minimum defines the optimum operating range for the system. Coincidentally, this pressure is also close to the maximum rated pressure for the rotary pump. Thus, the system is well designed for this application and the major components appear to match each other well. The motor current and feedwater flow are not plotted in Figure 16. They are both relatively independent of feedwater temperature and salinity and their variation with pressure was measured previously during pump testing (see Table IV and Figure 13).

Note the strong effect of feedwater temperature on system operation displayed in Figure 16. The permeate flow increases with temperature but the quality (salt rejection) suffers slightly. Clearly, the system operates more efficiently with warmer water. The RO elements are rated at a 25 °C temperature, but the water temperature in a typical application would more likely be between 5 and 20 °C. During testing, the recycled water warmed up from the power being dissipated in it. Thus, the actual temperature changed slightly as indicated in the figure.

In the next set of steady state tests, the feedwater temperature was fixed at about 21 °C and the salt concentration varied. The system was first flushed out with deionized water and tested without salt. Salt was then added to obtain 1000, 3000 and 5000 ppm NaCl by weight; the range of salinity found in brackish waters. For each concentration, testing was done as outlined above. The test results are presented in Figure 17. Note that the permeate flow lines are almost parallel, starting at different values of osmotic pressure. As expected, the specific energy increases with salt concentration, but not linearly. The salt rejection is meaningless for deionized feed water (no salt). At high pressures, it is almost the same for all three non-zero salinities.

Based on these test results, the nominal operating point for further testing was selected. The nominal system pressure was 1.45 MPa (210 psi). The feedwater concentration was 3000 ppm, at a temperature of about 20 °C. Some variation is expected due to changes in feedwater temperature and battery

voltage, but under these conditions, the permeate flow should be around 2.9 Lpm, giving a recovery fraction of about 38 %. The motor current under the same conditions should be about 18 A. These values are close to the system specifications (Table I) as well as the design characteristics (see Sections 4.2 and 6.6), indicating that the system is behaving as expected. For the remaining tests, the discharge valve was adjusted to give the nominal pressure with the correct feed water, and then fixed in place.

7.4 Transient Operation

Transient testing was performed to characterize the system startup and shutdown. The test started with the the PV array disconnected and the system off for more than two hours (it did not make any difference if the system had been off longer). The data loggers were set to record for twenty minutes and then started. They recorded the system pressure, battery voltage, motor current and permeate conductivity as described above. After one minute, the RO system was turned on manually. After ten minutes, with the system in steady state operation, the loggers were stopped and then restarted. After one minute, the system was turned off manually and the resulting transients recorded for a further nine minutes. The permeate and brine flows were not recorded since a single reading takes about 30 seconds. The resulting startup and shutdown transients are displayed in the plots shown in Figure 18. These plots were printed by a microcomputer running the data analysis software provided for the Rustrak Ranger data loggers. The plots also

indicate the conversion constants for each signal.

When the system is first started, the pump primes itself and clears out any bubbles in the plumbing. The motor current then rises as the pump pressurizes the stand pipe and RO elements. At the same time, the battery voltage drops due to its internal and wiring resistances. The brine starts flowing once the operating pressure is reached - about 12 seconds after startup. The permeate flow starts some 16 seconds later as the air is flushed out of the low-pressure side of the elements. The permeate conductivity does not change until the permeate starts flowing. Then it rises quickly as the stagnant permeate is flushed out. The salt concentration then drops more slowly as the stagnant water is diluted by fresh permeate. Note that even at the peak of the concentration plot, the water is still marginally acceptable for drinking. Since the old permeate is flushed out within two minutes, there is really no need for the permeate rejection solenoid.

The system reaches steady state after a few minutes. The pressure drops slightly at first and then levels off. Note the pressure spikes in the plot. These are caused by a micro water hammer effect in the pressure transducer whenever the pump clears air bubbles from the filter. As described above, these spikes caused high-pressure glitches in the control circuitry which would shut down the system in automatic mode.

There are two long-term transient effects not shown in the above plots. The motor heats up considerably during operation due to its internal losses (about 90 watts in steady state). From ambient temperature, the motor temperature rises toward a

value 50 °C above ambient with an exponential time constant of about 1.2 hours. Similarly, since the water is recycled and absorbs all the motor output power, it too heats up, toward a temperature some 15 °C above ambient, with an exponential time constant of about 6 hours. A plot of feedwater temperature vs time is shown in Section 7.5. This heating effect would not occur in a normal application where the permeate and brine would be separate from the feed water. In this test system, feedwater heating causes several effects. Permeate flow and salinity both increase and the specific energy decreases as indicated by Figure 16. As permeate flow increases, there is less brine through the discharge valve. The pressure control spring also heats up with the brine and the water viscosity decreases. The net effect is a steady drop in system pressure. This is also shown in Section 7.5.

The shutdown transient is more abrupt. Motor current, permeate and brine flow all stop immediately. The battery voltage rises abruptly without the resistance drop, and then slowly recovers toward a steady state open circuit voltage. The pressure decays quickly to a low value. Water dribbles out the brine discharge and leaks back through the pump as the air trapped in the system expands. The permeate is actually sucked back into the elements where it passes back through the membranes by osmosis. The resulting osmotic pressure decays slowly over a period of about 30 minutes. Air is sucked into the elements from the permeate discharge and displaces the water going backward through the membrane. At the same time, the remaining permeate in the elements becomes more

concentrated as brine diffuses into it through the membrane. When the air bubbles first reach the conductivity cell, the signal drops and then settles to a steady state value.

7.5 Long Term Automatic Operation

With the feedwater concentration and brine discharge valve fixed, the PV array connected and the data loggers operating, the RO system was placed in automatic. The loggers continuously recorded the solar irradiance, array current, battery voltage, system pressure and permeate conductivity. During daily operation, at irregular intervals, the system pressure, battery voltage, motor current, permeate flow and salinity, brine flow, feedwater temperature and salinity and motor temperature were manually measured and recorded. Table V lists sample results for one day along with several derived parameters: recovery fraction (Fr), salt rejection (R), specific permeate energy (Ep) and wire-to-water efficiency (..w-w). Note that the efficiency has improved slightly since initial pump testing (compare Table IV). This may be due to the warmer water or the pump may have "worn in".

Sample results for the most sunny day of automatic operation are presented in Figure 19. The solar irradiance, array current, battery voltage, system pressure and permeate conductivity plots were produced by the data analysis software. The data loggers were started around 8:30 that morning. The solar irradiance, array current and battery voltage prior to that were estimated on the basis of previously recorded data and sky observations. The permeate flow, motor current and

feedwater temperature were plotted manually, interpolating between the measured data points using the logged data and knowledge of the system operating characteristics based on Figures 16 and 17. From these results (Figure 19), the instantaneous effect of solar irradiance on battery voltage and system operation can be seen. The battery provides a good buffer to isolate the RO system from the changing sunlight conditions. Large changes in irradiance cause relatively small changes in voltage, current and flow.

Several other operating features are revealed in figure 19. The system starts up automatically when the battery charges up to about 26.5 V. Similarly, automatic shutdown occurs when the battery discharges to about 23.7 V as set in Section 5.3. The long term feedwater heating effects are clearly seen. The permeate flow increases throughout the day, the system pressure drops significantly and the conductivity increases as the water heats up and the salt concentration increases. On the conductivity plot, the initial startup transient is seen to be negligible over the day's operating period. By comparing the motor current and array current plots, it is seen that most of the time, the array current flows directly to the motor without any charge/discharge loss incurred in the battery. In fact, only about 15 % of the ampere hours from the array on this particular day actually see a charge/discharge cycle and the associated battery losses. Therefore, the system makes very efficient use of the available PV energy.

The system operated with data logging for eleven complete days, ten of them contiguous. Each day's results were stored on

diskette and analysed using the loggers' software package as well as manual analysis. The solar irradiance, array current, motor current and permeate flow signals were all integrated. The average specific energy (kilojoules of motor drive energy per litre of permeate) for that day and the average overall system productivity (litres of permeate per MJ/m^2 of insolation) were also calculated. The results are summarized in Table VI. On the first two days, the system was started manually, having previously been off and trickle charging. For this reason, their results are not included in the averages shown in the bottom row of the table. Thereafter, the system ran automatically. Note the wide range of operating periods, loosely correlated with the insolation for each day. On three days, the system did not start up at all due to low sunlight conditions, but the battery charging did contribute to the next day's operation.

Because of feedwater heating, most of the net permeate volumes are unrealistically high. Similarly, the specific energy obtained in a real application is likely to be higher than most of those shown; the values for Oct. 24 and 28 are more representative as the water did not have a chance to heat up very much on those days. These results are close to the 10 kJ/L value predicted in Section 6.6. The data for Oct. 26 are closest to the design day of 18 MJ/m^2. Even accounting for the high water temperature, it is clear that the goal of 1000 litres per day for such a day has been met.

Using the logged data, the battery cycling for each day can be estimated. It is difficult to determine the absolute

state of charge of the battery since it's starting capacity was not known, but the relative, day-to-day ampere hour charging and discharging can be estimated. The battery appears to be operating around 50% of its capacity, with an average discharge cycle depth (on operating days only) of about 12 %. This implies that, as mentioned above, the array output is being used efficiently, with only a small amount of the total energy being stored, and also, that the 165 AH battery capacity is adequate for this system.

8. EVALUATION AND DISCUSSION

8.1 Evaluation of Prototype System

Based on the above test results, the prototype PV/RO system appears to function very well. It performed as expected, close to the calculated operating point. The components in the system are well matched to each other and well suited to the specified application in that their optimal operating points are all close to each other and to the required values. There was more variation in the operating point than anticipated, mostly due to heating of the recycled feedwater and its strong effect on permeate flow and system pressure.

During testing, the array, batteries, voltage regulator, motor, pump, plumbing and RO elements all worked well, without problems. The only problems encountered were with the control logic circuit. The false high and low pressure shutdowns are discussed further in section 8.2. Another minor problem was discovered only when the system had been left off for several days. When started up, the first bit of permeate appeared rusty. When the system is off, the permeate, with its residual salt is stagnant in the conductivity cell. The cell remains connected to the control circuit DC supply, however, resulting in some hydrolysis or other electrochemical reactions in the cell. This causes some rusting of the stainless steel electrodes and also contaminates a small amount of permeate. When the cell was disconnected from the controller, the rusting did not occur.

The weak point in the system is still probably the pump. With an efficiency of only 46 to 50 %, it wastes a lot of the

valuable PV power. High quality piston pumps with efficiencies of 60 to 80 % are available. An increase of 20 % in efficiency would save about 125 W of electrical power. At $10 per peak watt for PV modules, the pump could cost three or four times as much and still be cost effective!

The total cost of the prototype system hardware was about $16,000 Cdn. The PV array cost is around $10,000 while the RO elements and pressure vessels cost about $3350. The balance is the cost of the pump, motor, plumbing, controller and other hardware. The system should operate for about three to five years without major replacement costs. At that time, the RO elements, batteries, motor and pump would likely all need to be replaced. Over five years then, with 1000 to 1200 litres per day of permeate in a typical, sunny location, the cost of product water would be about $8 per cubic meter, or less than one cent per litre. In a commercial product, of course, labour, packaging and profit would have to be added to this cost. On the other hand, most of the capital equipment (eg. the array and the pressure vessels) should last much longer than five years and most of the components would be less expensive in quantity.

The system should require minimal maintenance. The pump and motor require no lubrication. The PV array and control electronics should not need any attention. Only the filter and RO elements need to be checked and replaced if necessary. Their frequency of cleaning or replacement will depend entirely on the quality of the feedwater. The filter cartridge is inexpensive and could be changed frequently if necessary. If

the water is properly filtered, the RO membranes should not become clogged, and should last several years. The elements do not normally fail abruptly, rather the permeate flow slowly decreases as the micropores clog up. When this occurs, the elements can sometimes be rejuvenated by backwashing them with a high flow of clean water.

8.2 System Redesign

Although the PV/RO system functioned well, it is only a laboratory prototype. There is still much development work required before a complete and dependable system can be produced, sold and placed in the field. Some changes are needed in the basic design of the system. Alternatives to the Procon rotary pump should be examined, especially some of the high quality piston pumps. In any non-laboratory application, a feedwater pump is necessary. Small, low-flow centrifugal pumps should be investigated for this purpose. Depending on the type of pump selected, the standpipe may not be necessary or may have to be moved to the main pump inlet. In many applications, the conductivity cell and permeate reject solenoid may not be required. This would simplify the system somewhat. On the other hand, some systems may require additional features such as a backwash cycle controller or status displays. Finally, for outdoor use, a robust support frame and mounting structure with enclosure are essential. These should be designed for ease of transport and installation.

Several of the design changes involve the system controller. The pressure pulses which cause false high-pressure

shutdowns could easily be filtered out at the input from the pressure transducer (see figure 7) using a low-pass filter. To solve the problem of setting the low-pressure alarm during normal system shutdown, the corresponding flip flop in the control circuit should be reset whenever the pump is not operating. This would have to be done carefully, however, to avoid resetting after a valid low-pressure shutdown. Alternatively, since an abnormally low pressure is not a safety hazard, it may be better to do away with this part of the circuit altogether.

Power to the conductivity cell should be cut when the pump is off to avoid contaminating the stagnant permeate and possibly rusting the cell. The battery voltage thresholds which control the automatic startup and shutdown of the system should be adjusted to cycle the battery at a higher state of charge. At present, the battery appears to be cycling around a 50 % state of charge, which is somewhat low. Finally, the controls and power regulator should be combined on a dedicated printed circuit board with appropriate connectors for the sensors, actuators and power components which would be mounted off the board.

In most brackish water treatment applications, the water is less benign than the NaCl solution used in this project. Water hardness, organic silt and silica particles reduce the efficiency and life of the RO membranes. In many cases, various forms of feedwater pretreatment such as water softening or fine filtration are required. This of course would add to the system cost and electrical load. Other simpler forms of additional

treatment are possible. An ultra-violet sterilization cell, similar to the one recently developed by TPK, could be added at the inlet to kill micro-organisms [10]. It is a good idea in drinking water systems to add an activated carbon filter at the product water outlet to improve the taste.

Because there is great variation among brackish waters, the RO system has to be customized to each particular site. The type and size of the elements used as well as the feedwater pretreatment, operating pressure and recovery fraction have to be selected on the basis of a water sample analysis. To ensure that future RO systems are well designed for the particular application, TPK should team up with a water treatment company to benefit from their experience in this area.

Two design enhancements should be considered to improve the performance of future systems. The energy released in the brine discharge valve represents over 50 % of the hydraulic energy of the pump. If this could be recovered hydraulically or mechanically with a good efficiency, it would substantially improve the overall system efficiency and would likely be cost effective. The key is to discover an inexpensive, yet reliable means for doing this. A second possibility is to heat the incoming feedwater to increase the recovery fraction of the RO elements at a given pressure. This could be done in principle using a suitable heat exchanger to utilize the heat generated in the PV array. Another exchanger could recover some of the heat from the warm brine and/or permeate flows. The water could be heated as much as 1[illegible] °C in this way which would reduce the energy required per litre of permeate. The PV array would also operate at a lower temperature and thus, more efficiently.

9. CONCLUSIONS AND RECOMMENDATIONS

The project has been very successful. A prototype photovoltaic powered reverse osmosis system for desalinating brackish water was developed using commercially available components. The major components were tested and found to function as expected. The PV/RO system was assembled and tested in transient and steady state operation under a range of operating conditions. The system performed as expected and all of the design goals were met. During the development, a lot was learned about reverse osmosis in general, and photovoltaic powered desalination in particular. A substantial potential market exists for such systems in remote areas of the world where no potable water or grid power is available.

The prototype system operates best at a pressure around 1.4 MPa. Some 38 % of the brackish feed water, containing 1000 to 5000 ppm of dissolved salts, is recovered as potable product water with 98 % of the salt removed. This water is produced at a flow of about 3 Lpm which varies with pressure, temperature and salinity. The system draws some 430 watts from the 24 V battery when operating. The battery is charged by a 740 watt PV array whenever the sun is shining. With a typical daily insolation of 18 MJ/m^2, the system produces over 1000 litres of drinking water at an energy cost below 10 kJ/L. The design is quite flexible and could be readily scaled up or down for different PV power levels.

The present system is only a laboratory prototype. Considerable development work remains to be done before a system based on this design can be ready for field use in a

real application. The basic RO system can be improved in several ways. The electronic controller must be redesigned, and additional features should be added for long term, trouble-free operation at a remote site. For the purpose of correctly selecting RO elements, operating points and feedwater pretreatment techniques in particular applications, TPK should team up with a water treatment company with expertise in this area.

It is also recommended that, following further development of the design, and prior to marketing in developing countries, a complete system be subjected to field trials in Canada. Such trials would provide a wealth of experience in installation, maintenance and real-world operation of PV/RO systems. The systems could also be monitored to collect valuable performance data and to assess their reliability in the long term. Following this, TPK could confidently go to the market with dependable and economical desalination systems for use in remote areas of Canada and the rest of the world.

REFERENCES

[1] R.H. Perry and C.H. Chilton, Chemical Engineer's Handbook, 5'th edition, McGraw-Hill, 1973, pp. 17-40 to 17-43.

[2] T.I. Hedrick, "Reverse osmosis and ultrafiltration in the food industry: Review", Drying Technology, 2 (3), 1984, pp. 329-352.

[3] B.G. Keefer, R.D. Hembree and F.C. Schrack, "Optimised matching of solar photovoltaic power with reverse osmosis desalination", Desalination, 54 (1985), pp. 89-103.

[4] C.E. Norman, W. MacKeigan and D.G. MacKenzie, "Development of a photovoltaic power supply and microprocessor controller for a reverse osmosis water desalination system", Final Report to Highquest Engineering for a DSS/NRC contract, April 1985.

[5] For recent work on RO membrane technology, see proceedings of the International Membrane Conference, Ottawa, September 1986.

[6] C.E. Norman, D.G. MacKenzie and P.S. Harris, "Test and evaluate high-efficiency, modular power conditioning systems for photovoltaics", Final Report DSS/NRC Contract No. OSX82-00049, July 1984.

[7] C.E. Norman, C. Robins and B.G. Keefer, "Development of a photovoltaic powered shallow well pumping system", Final Report DSS/NRC Contract No. OSX83-00162, Nov. 1984.

[8] C.E. Norman, C. Robins and D.G. MacKenzie, "Photovoltaic water pump development", Final Report on Technical Development, Ontario Ministry of Energy Contract No. 809-8205, August 1984.

[9] "Omega 1987 complete pH and conductivity measurement handbook and encyclopedia", Omega Engineering, Stamford, Conn., U.S.A., 1987, pp. A10 -12.

[10] C.E. Norman, "Development of photovoltaic powered ultraviolet water treatment system", Final Report, DSS/EMR Contract No.1SZ85-00188, March 1987.

APPENDIX A

FIGURES AND TABLES

LIST OF FIGURES AND TABLES

FIGURES

Figure 1. Steady state operating characteristics of typical thin-film composite RO membranes.

Figure 2. Typical RO Systems: a) single-pass, multi-element; b) single-element, recirculating.

Figure 3. Block diagram and operation of a battery based PV powered reverse osmosis system.

Figure 4. Block diagram and operation of a maximum power tracker based PV/RO system.

Figure 5. Hydraulic operating parameters for an RO system consisting of three TW30-2540 elements in series.

Figure 6. Prototype photovoltaic-powered reverse osmosis system for brackish water.

Figure 7. Control circuit for prototype PV/RO system.

Figure 8. Modifications made to VR-24S circuit for use in PV/RO system.

Figure 9. Prototype power regulator and controller for the PV/RO system.

Figure 10. Prototype photovoltaic-powered reverse-osmosis system.

Figure 11. Steady state operating characteristics of Pacific Scientific 24 VDC, permanent magnet motor Model No. BA3628-7012-9-48B, rated at 1/2 HP, 1800 RPM.

Figure 12. Characteristics of the Hypro 5320BHR piston pump operated at 1800 RPM.

Figure 13. Measured characteristics for the Procon 2502 rotary pump, operating at 1800 RPM.

Figure 14. Pressure-flow characteristics for the three TW30-2540 elements used in the prototype PV/RO system.

Figure 15. Monitoring instrumentation for the prototype PV/RO system.

Figure 16. Performance of PV/RO system with varying feedwater temperature.

Figure 17. Performance of PV/RO system with varying feedwater concentration.

Figure 18. Startup (left) and shutdown (right) transients for the prototype PV/RO system.

Figure 19. Prototype PV/RO system operating data for October 26, 1987.

TABLES

Table I. RO System Specifications.

Table II. Comparison between two types of power conditioning for RO systems.

Table III. Test results for Hypro 5320 BHR piston pump.

Table IV. Test results for the Procon 2502 rotary pump.

Table V. Sample of operating data and derived performance parameters for the prototype PV/RO system in automatic operation on Oct. 21, 1987.

Table VI. Summary of performance of prototype PV/RO system during eleven day operating trial in October, 1987.

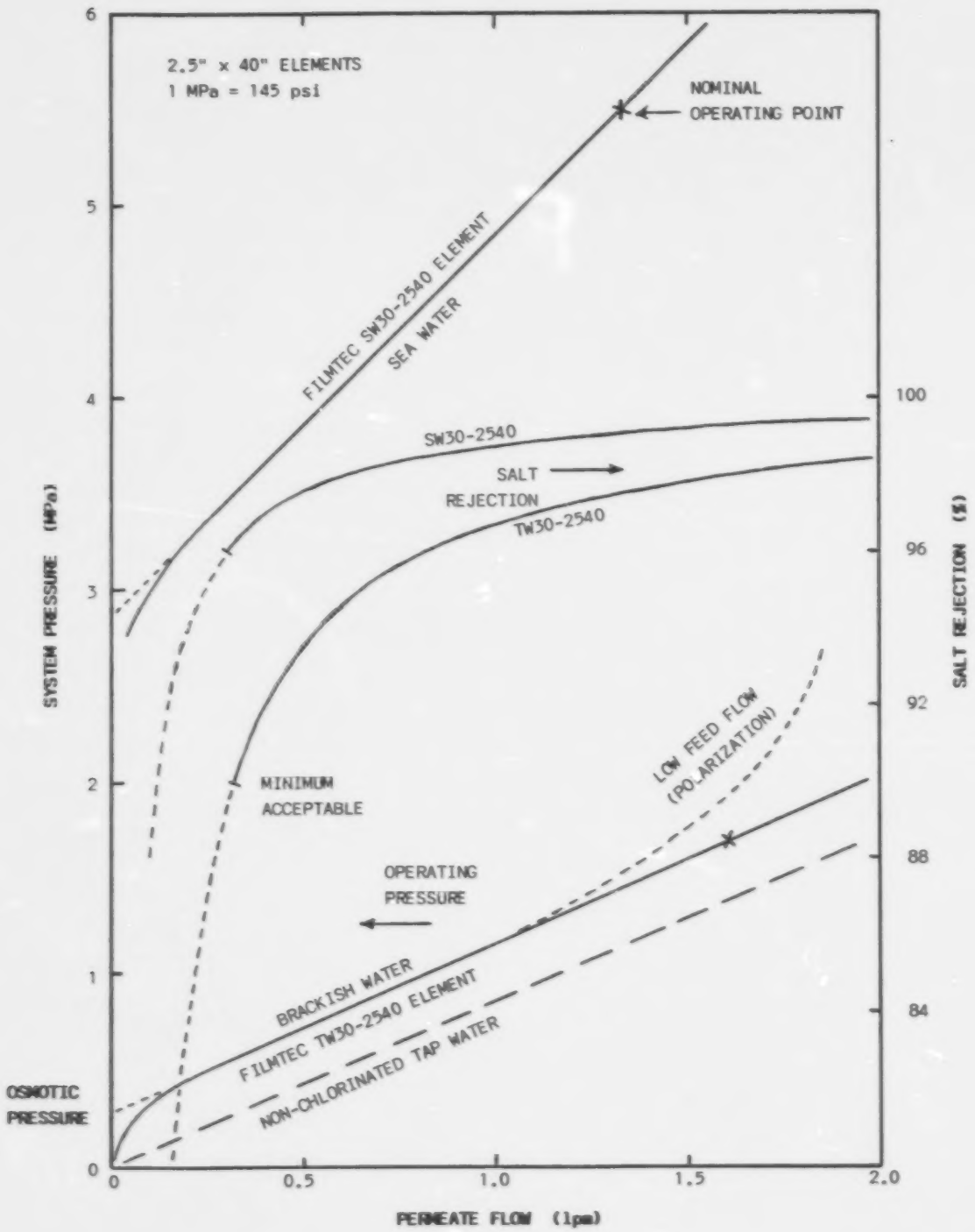

Figure 1. Steady state operating characteristics of typical thin-film composite RO membranes.

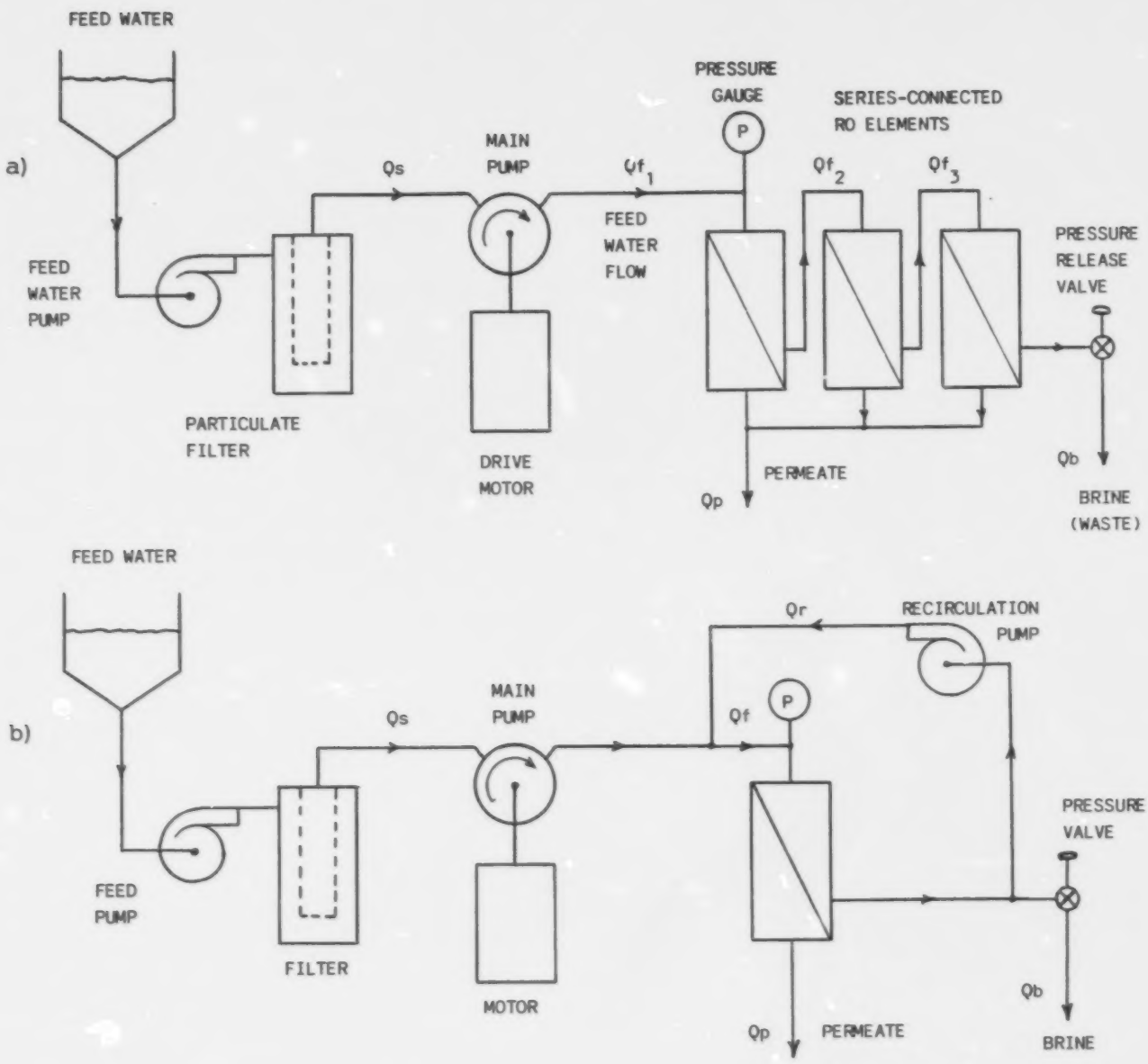

Figure 2. Typical RO Systems:

a) single-pass, multi-element
b) single-element, recirculating

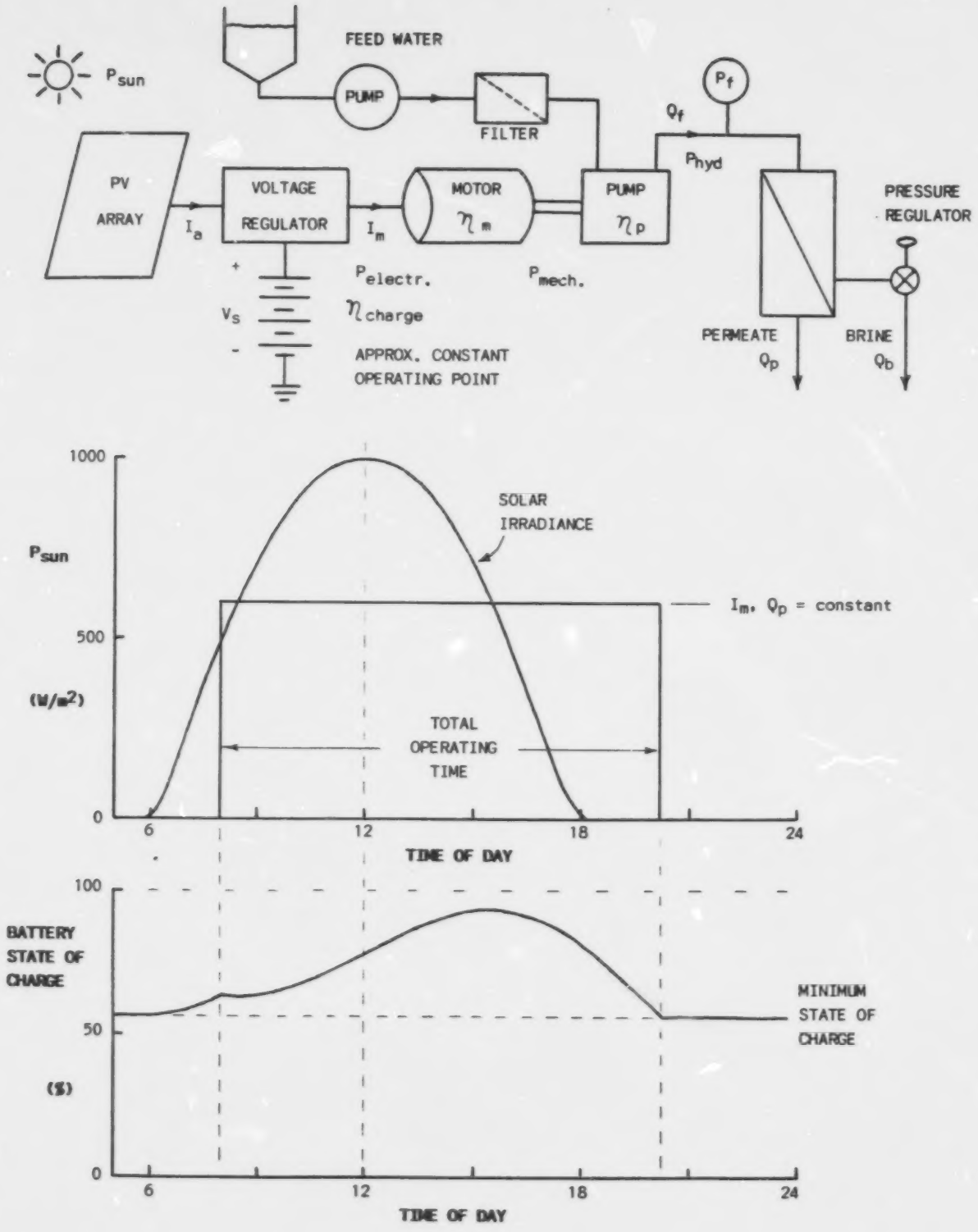

Figure 3. Block diagram and operation of a battery based PV powered reverse osmosis system.

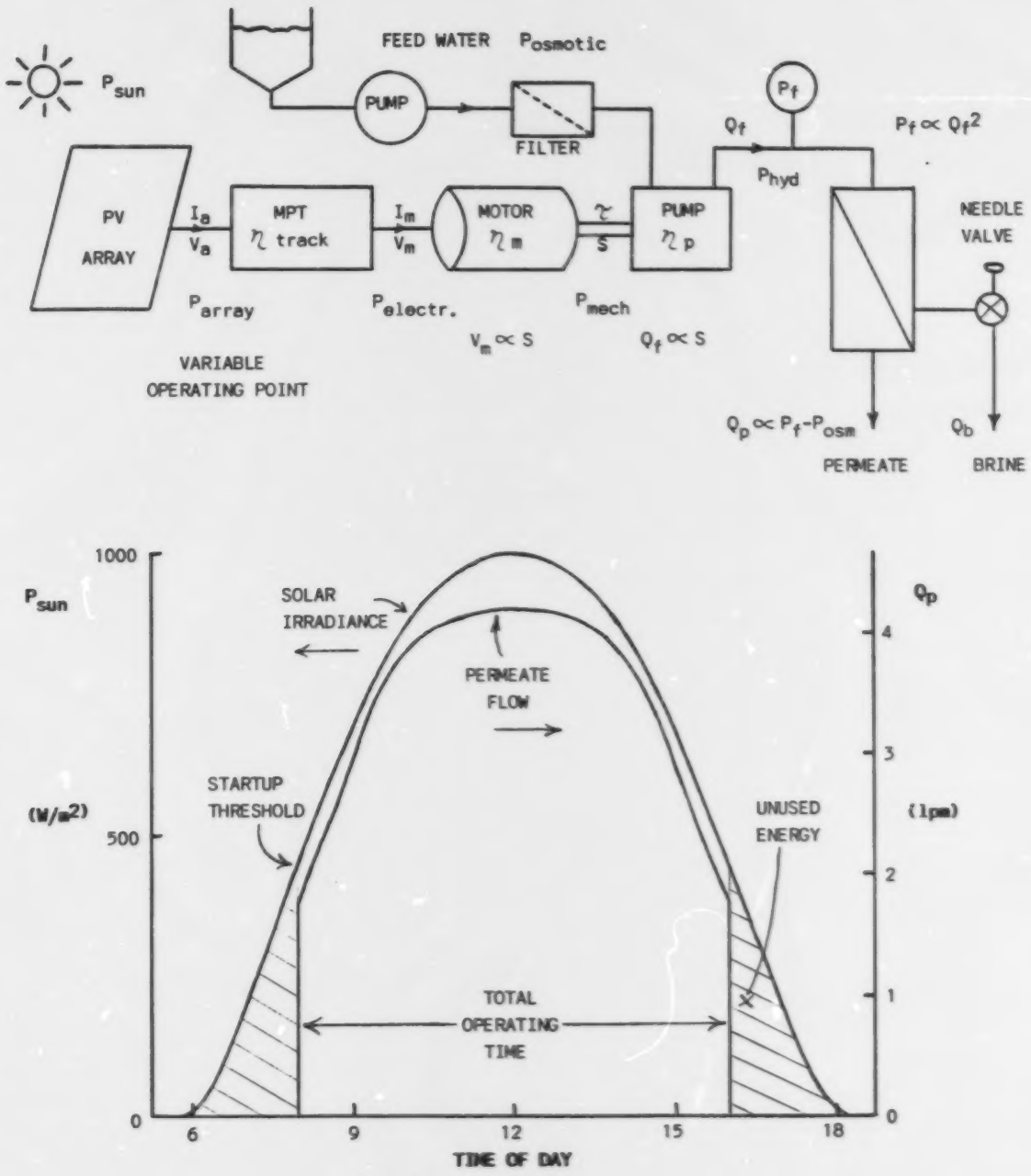

Figure 4. Block diagram and operation of a maximum power tracker based PV/RO system.

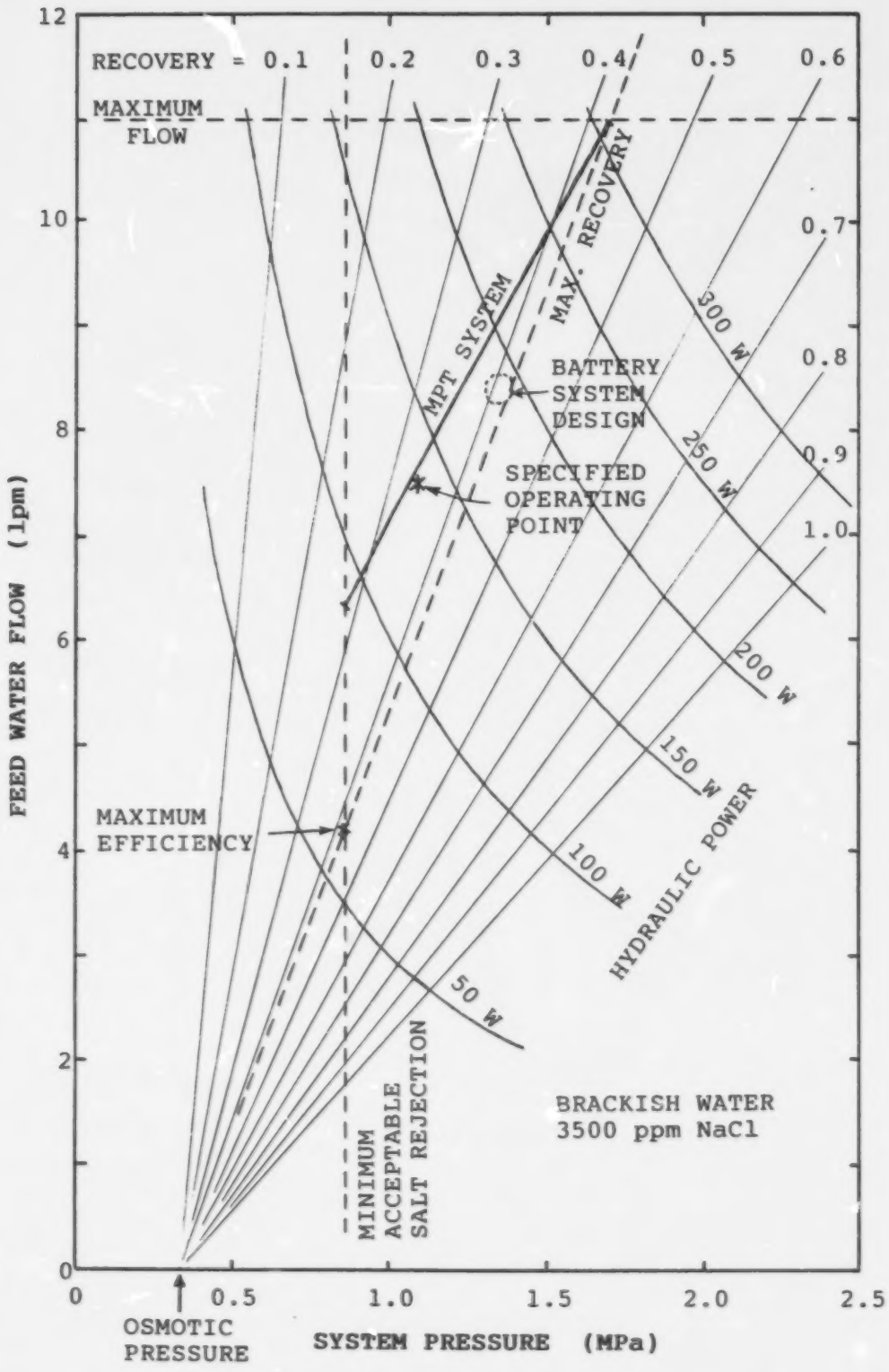

Figure 5. Hydraulic operating parameters for an RO system consisting of three TW30-2540 elements in series.

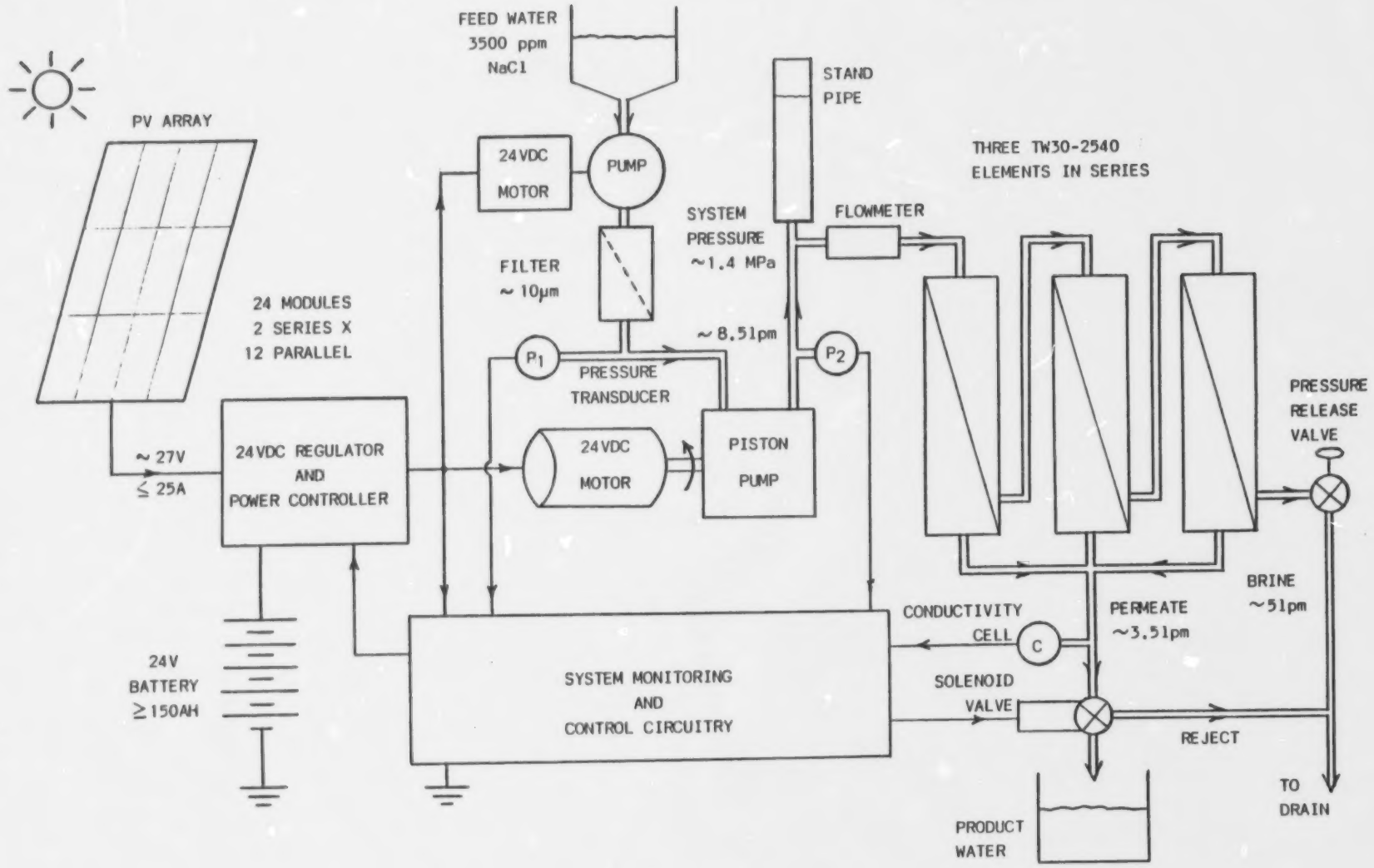

Figure 6. Prototype photovoltaic-powered reverse osmosis system for brackish water.

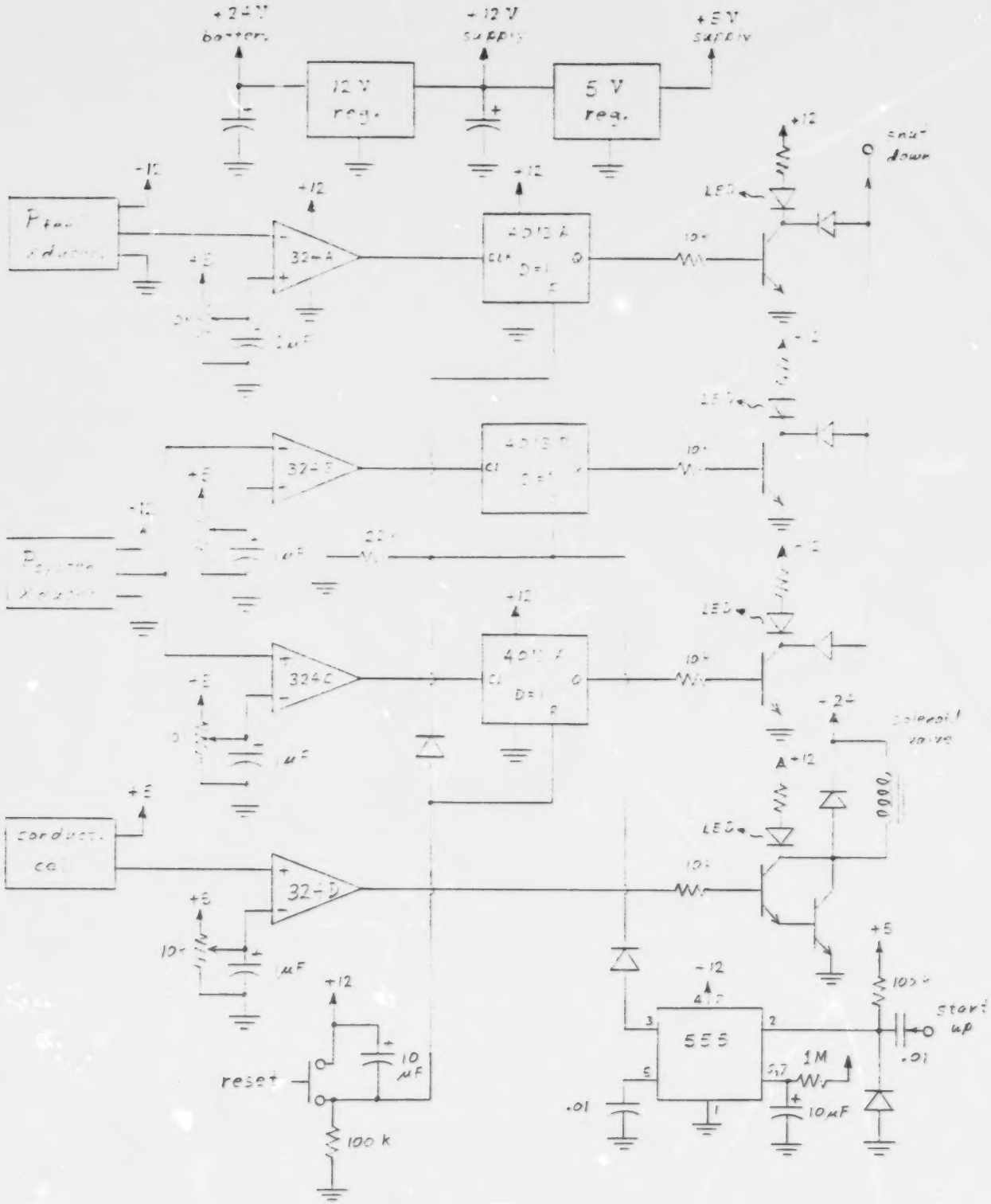

Figure 7. Control circuit for prototype PV/RO system.

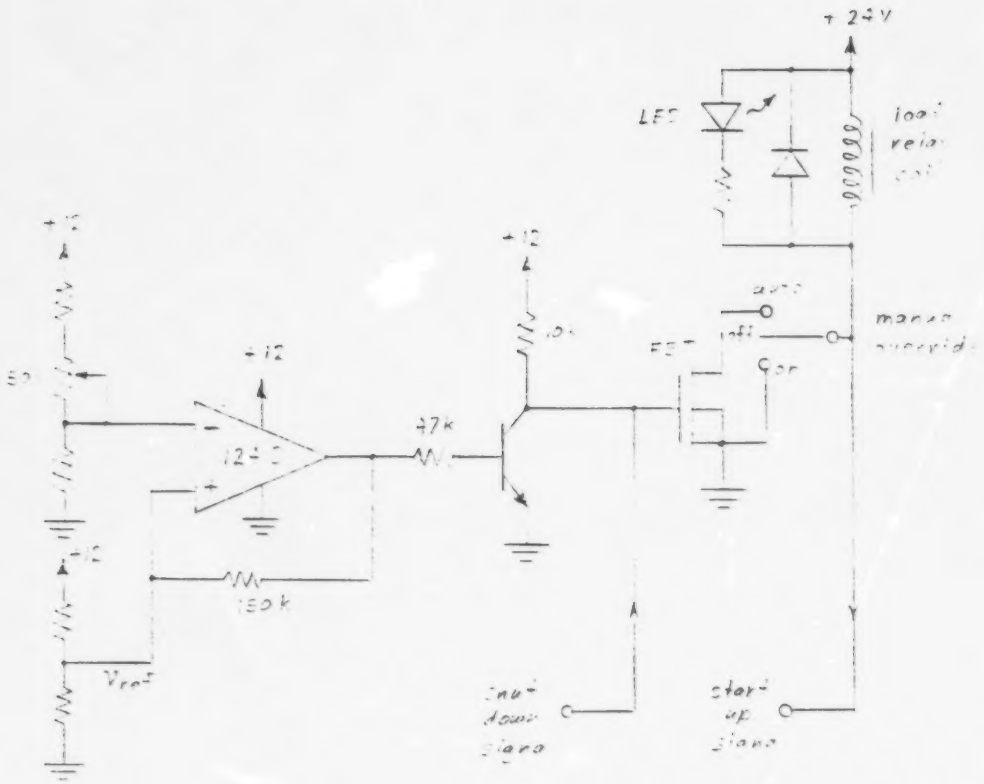

Figure 8. Modifications made to VR-24S circuit for use in PV/RO system.

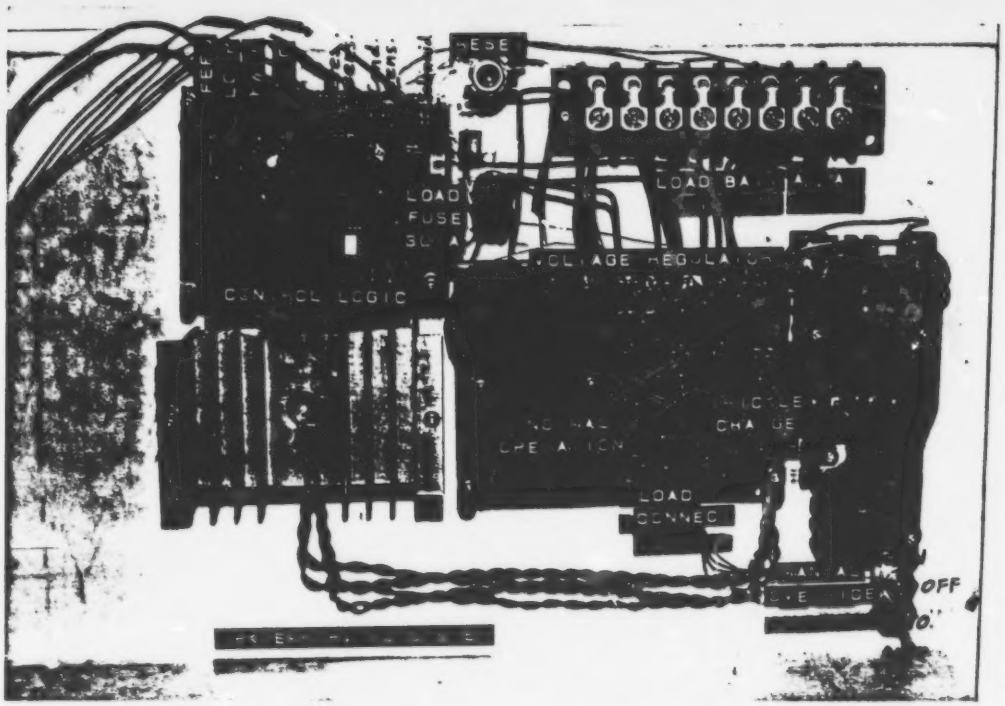

Front View

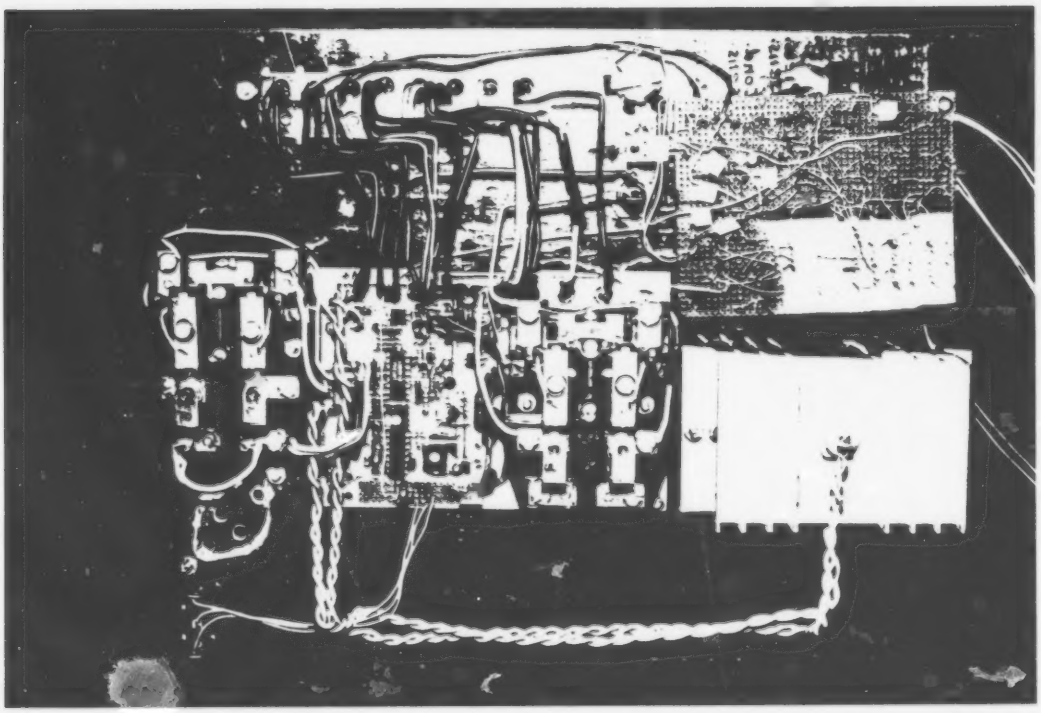

Back View

Figure 9. Prototype power regulator and controller for the PV/RO system.

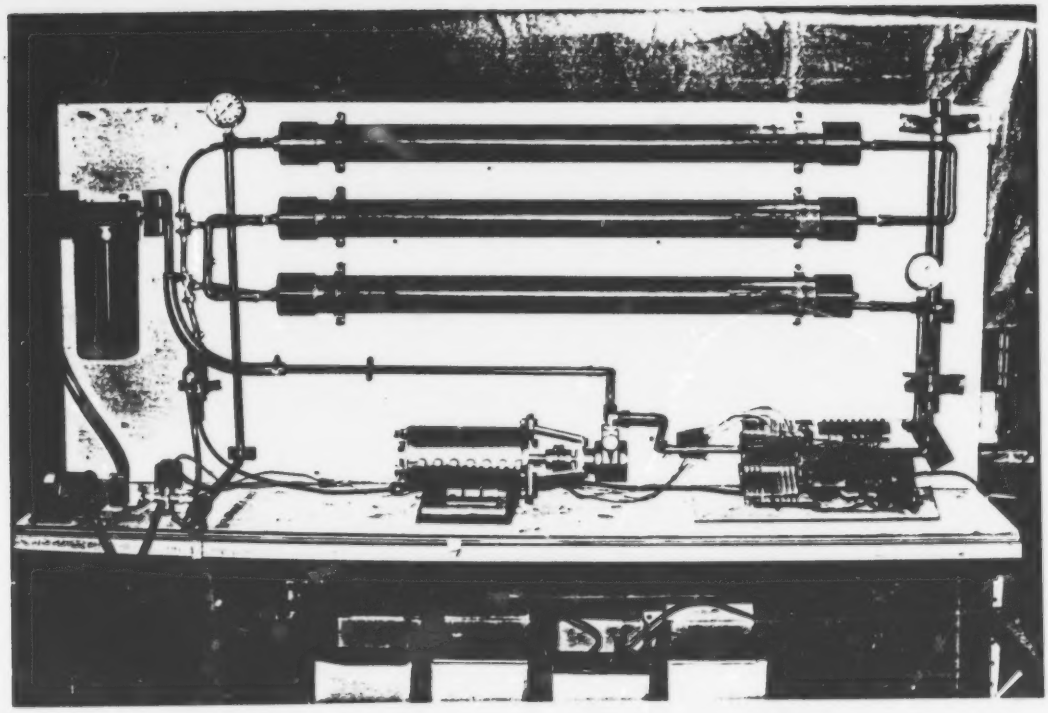

RO System

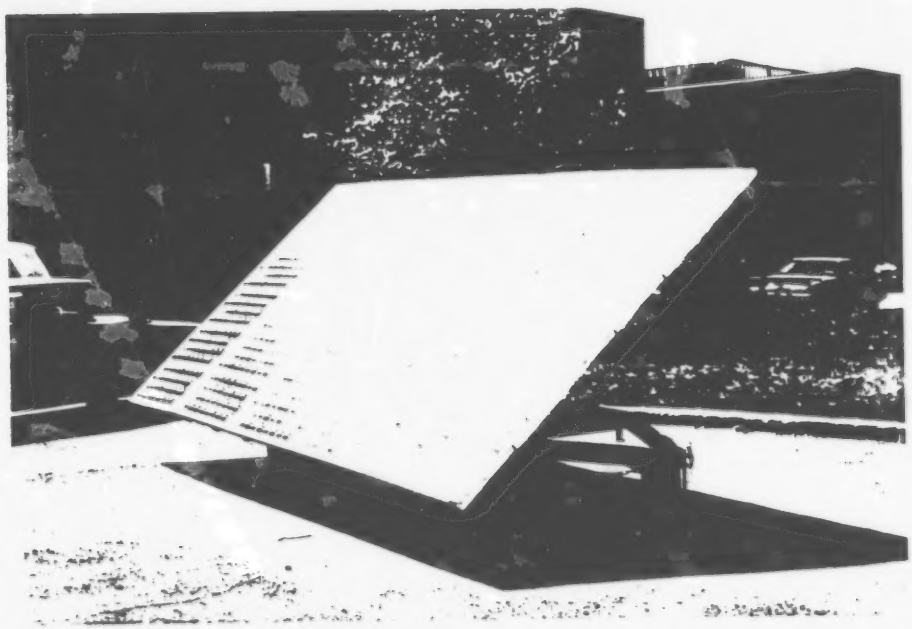

Trailer Mounted PV Array

Figure 10. Prototype photovoltaic-powered reverse-osmosis system.

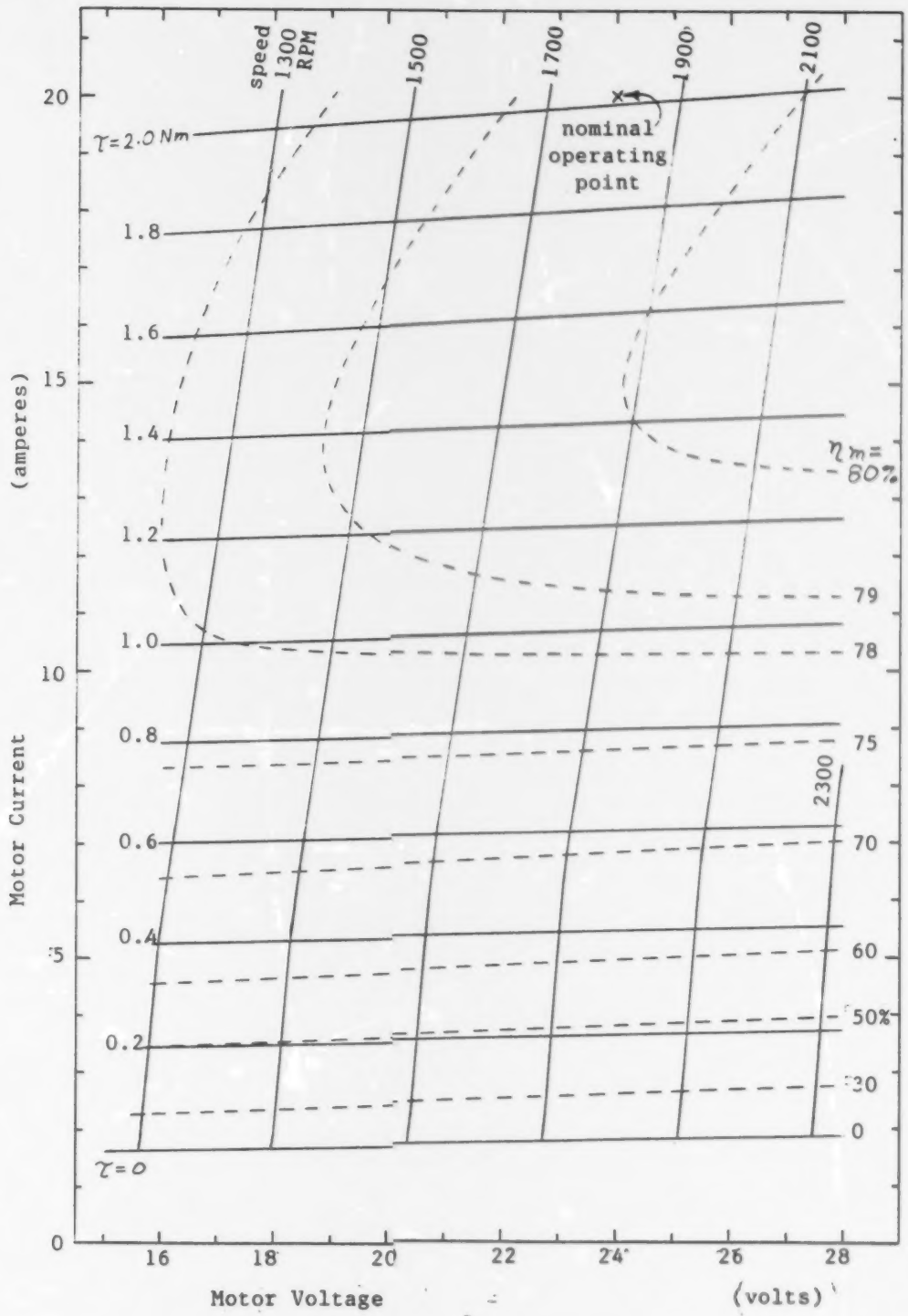

Figure 11. Steady state operating characteristics of Pacific Scientific 24 VDC, permanent magnet motor Model No. BA3628-7012-9-48B, rated at 1/2 HP, 1800 RPM.

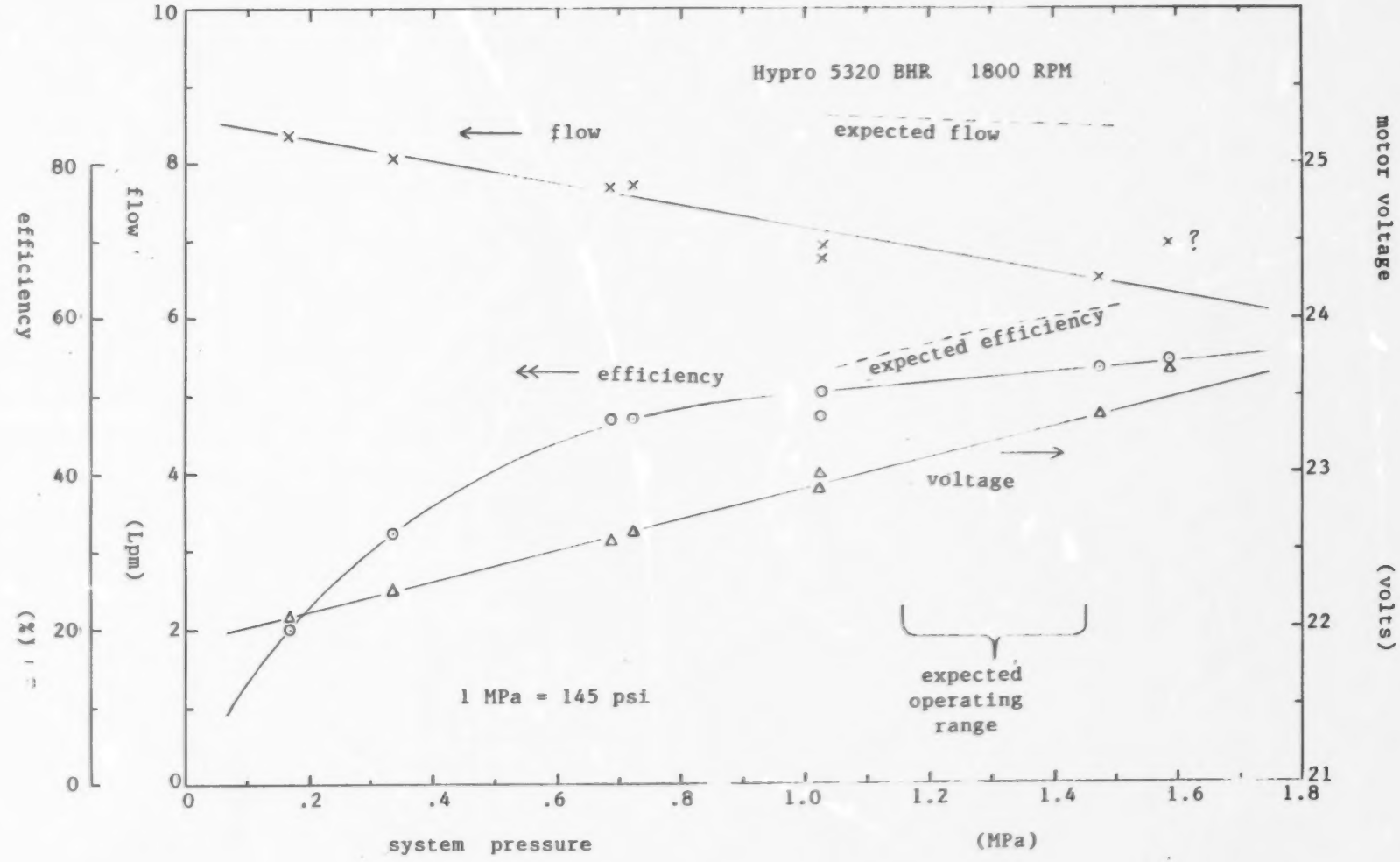

Figure 12. Characteristics of the Hypro 5320BHR piston pump operated at 1800 RPM.

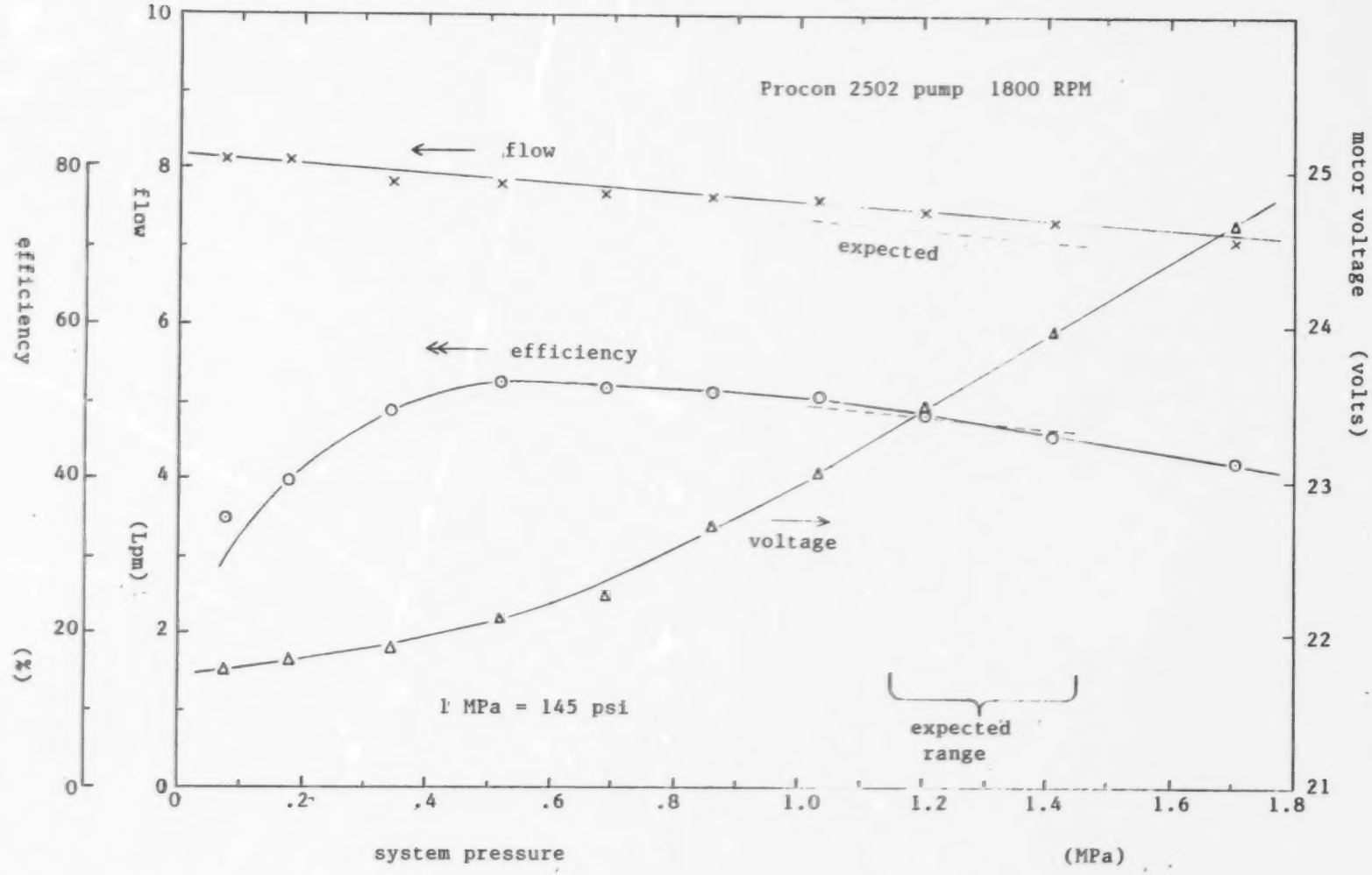

Figure 13. Measured characteristics for the Procon 2502 rotary pump, operating at 1800 RPM.

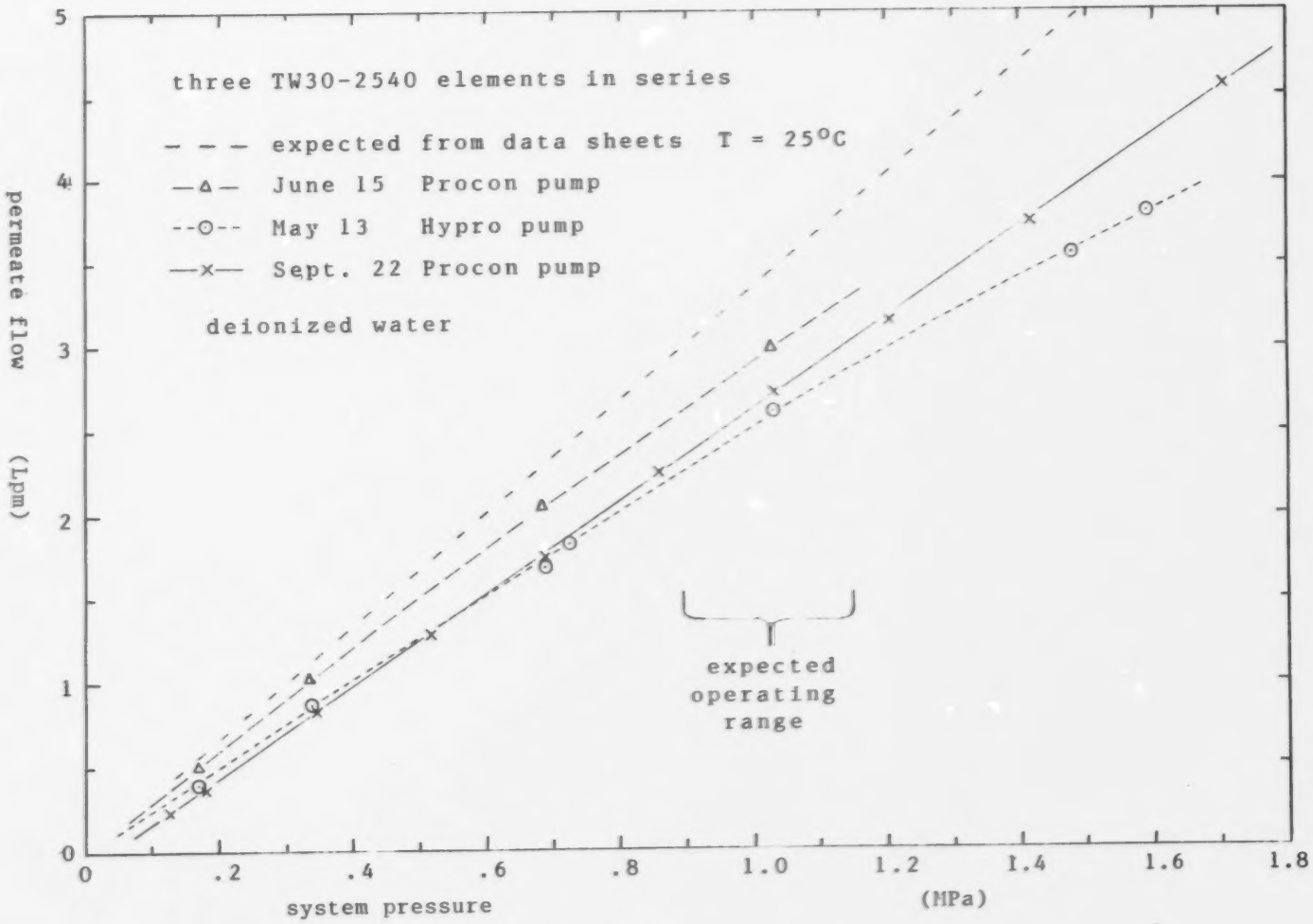

Figure 14. Pressure-flow characteristics for the three TW30-2540 elements used in the prototype PV/RO system.

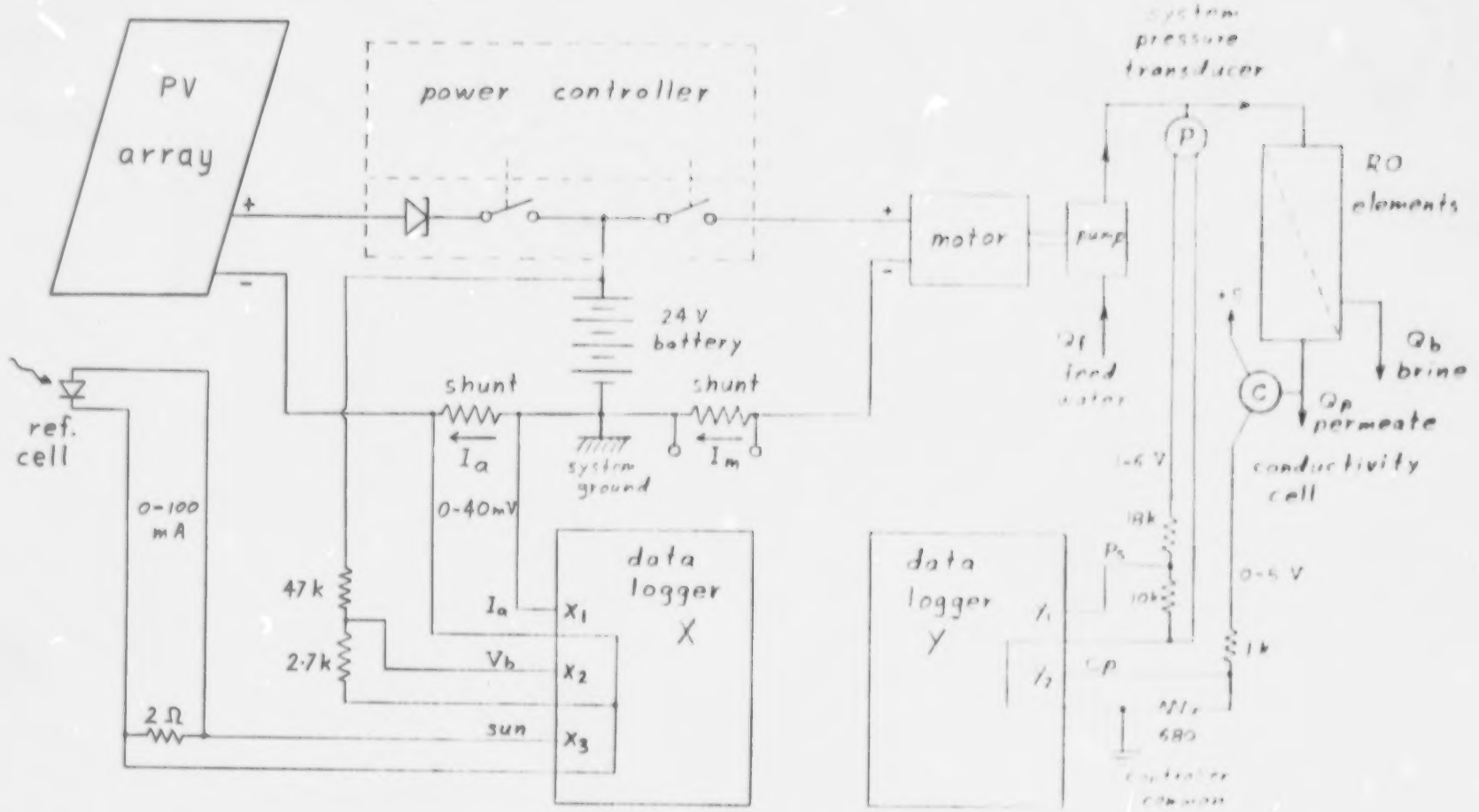

Figure 15. Monitoring instrumentation for the prototype PV/RO system.

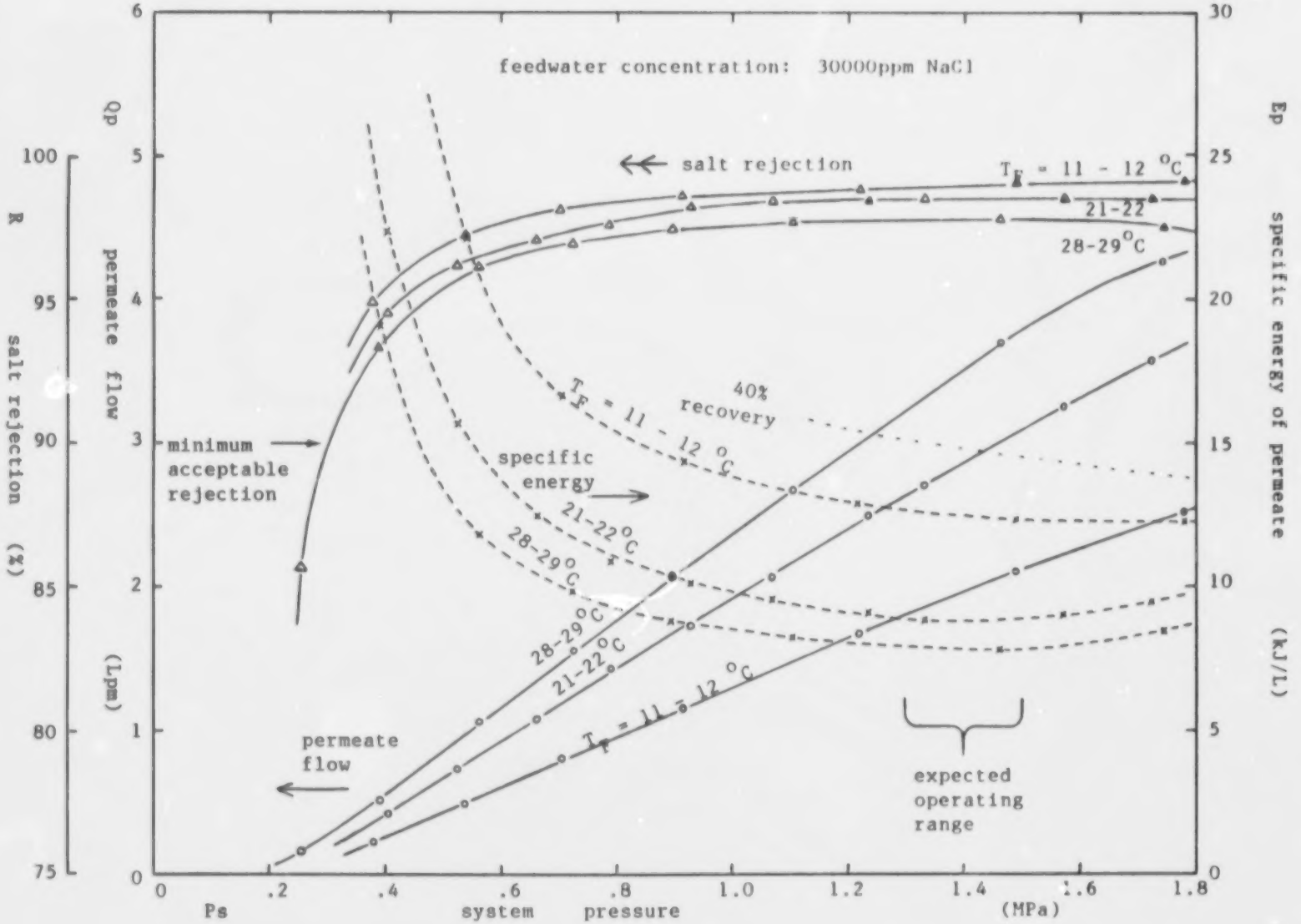

Figure 16. Performance of PV/RO system with varying feedwater temperature.

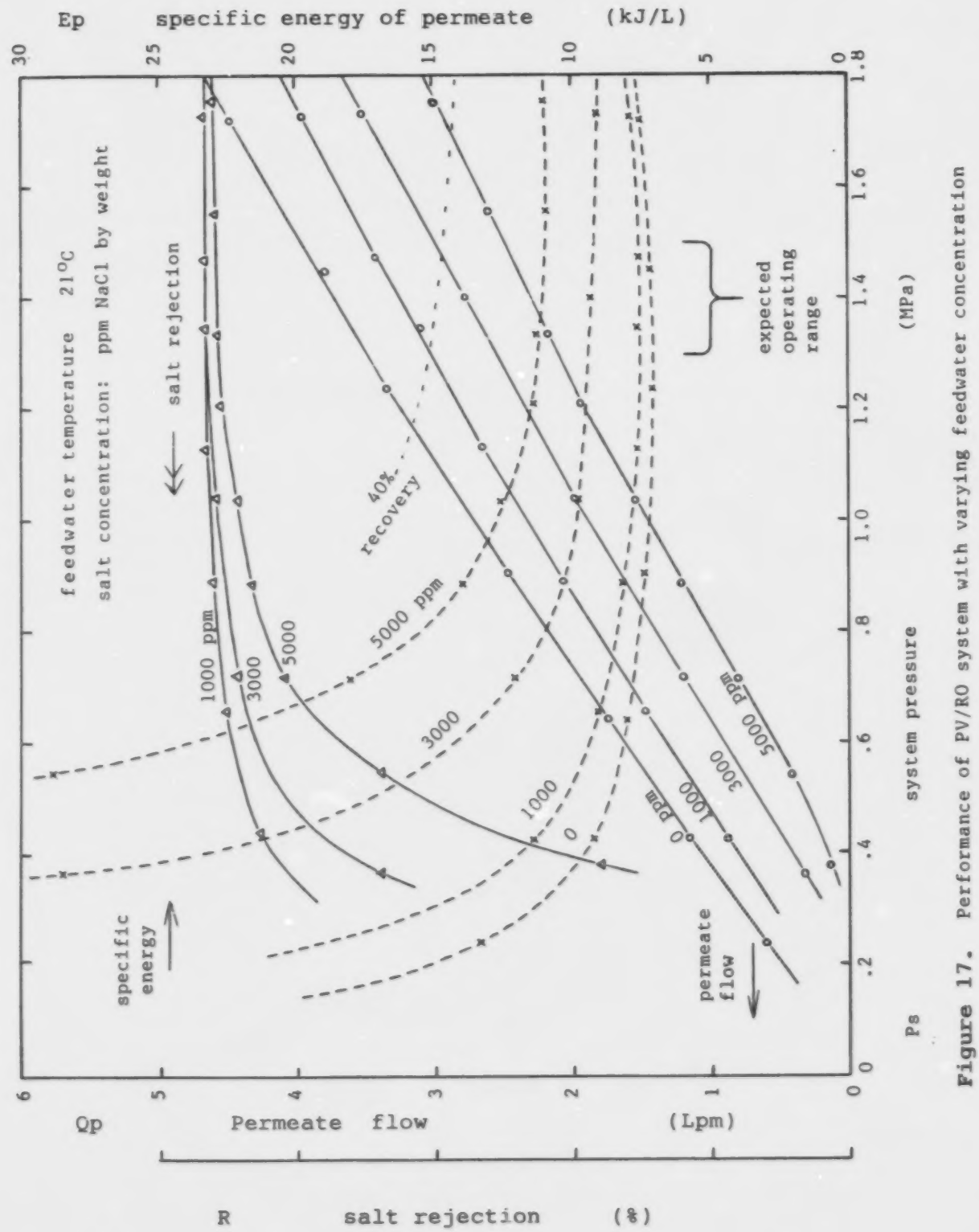

Figure 17. Performance of PV/RO system with varying feedwater concentration

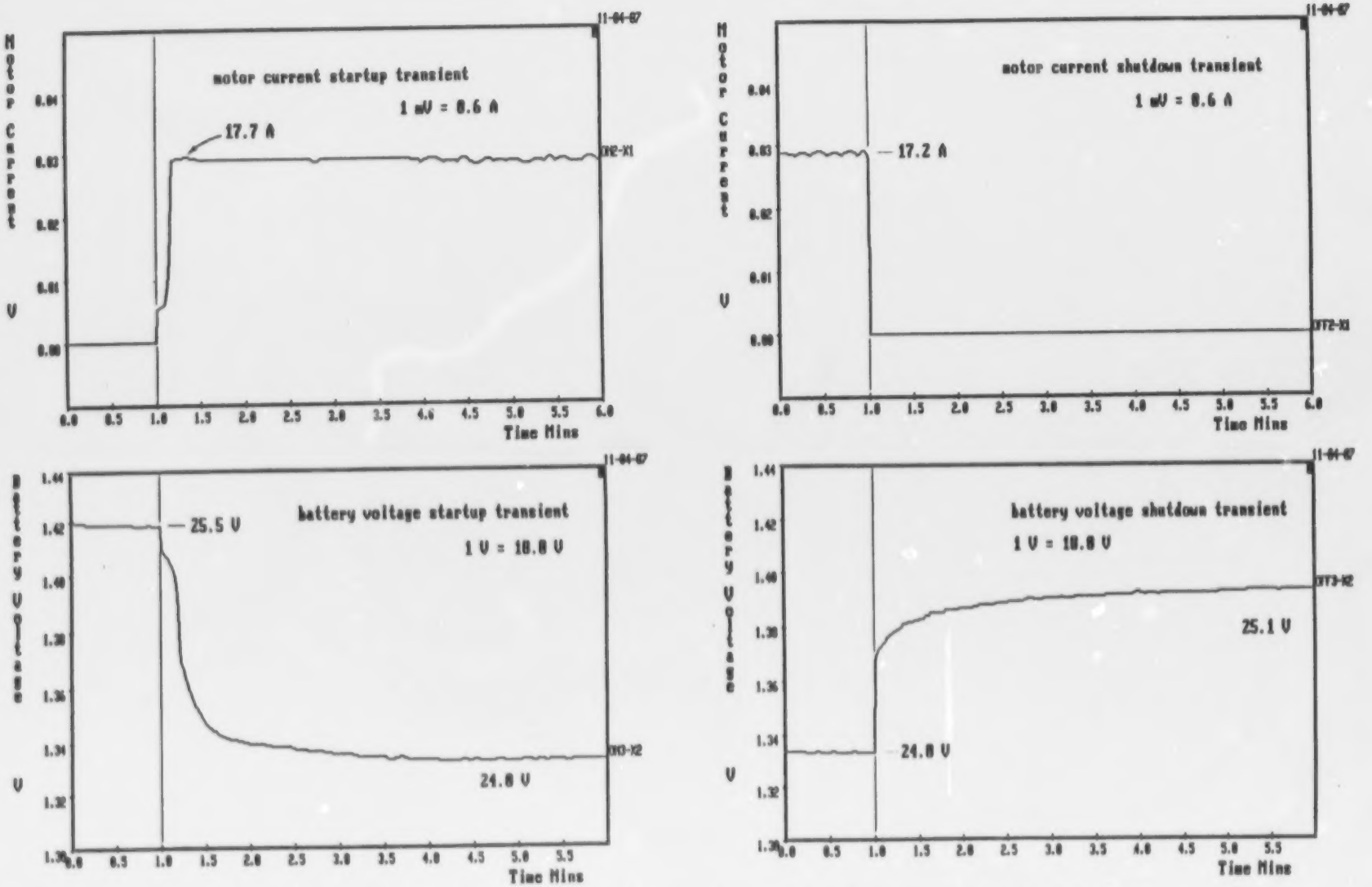

Figure 18. Startup (left) and shutdown (right) transients for the prototype PV/RO system. Both startup and shutdown occur at 1.0 minute on time axis.

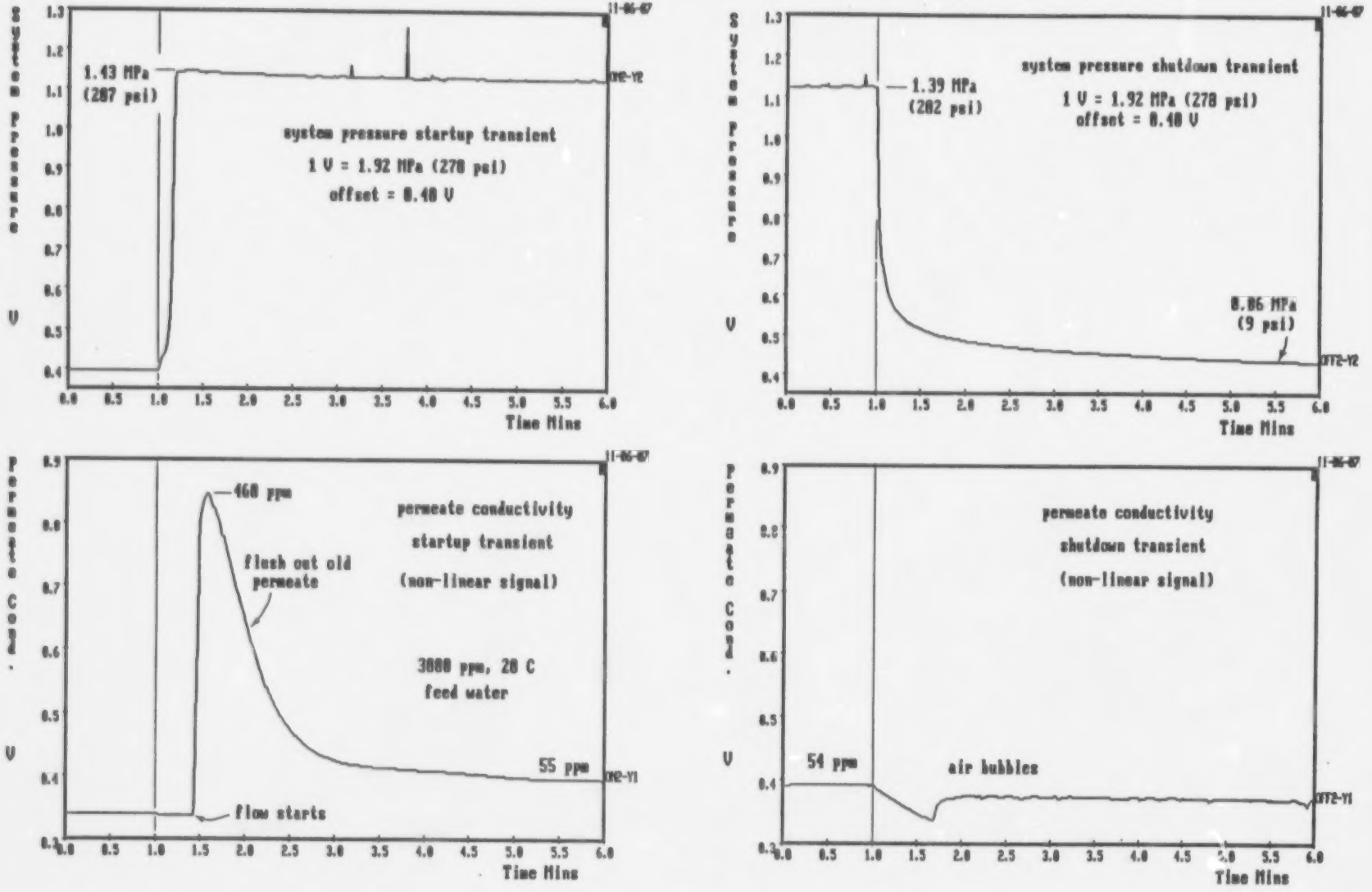

Figure 18. Startup (left)and shutdown (right) transients (continued).

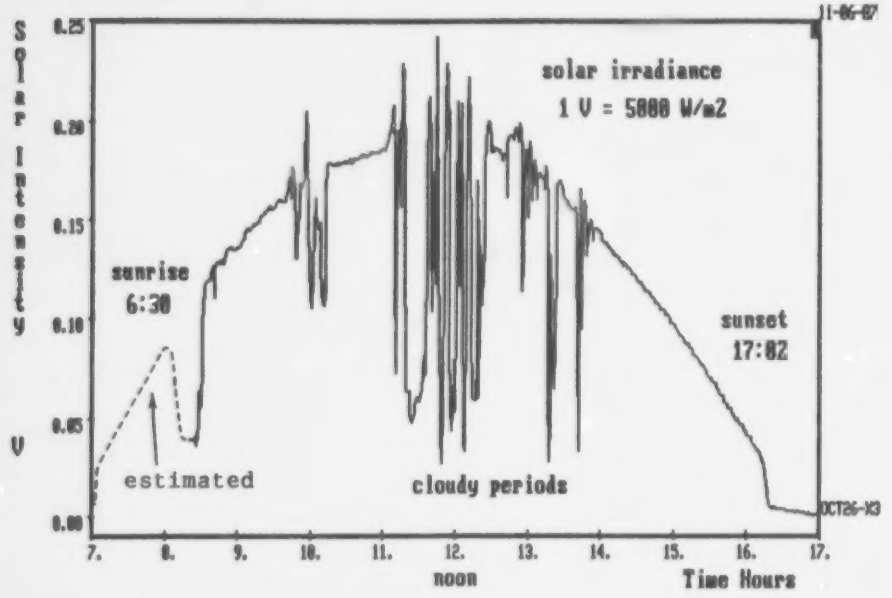

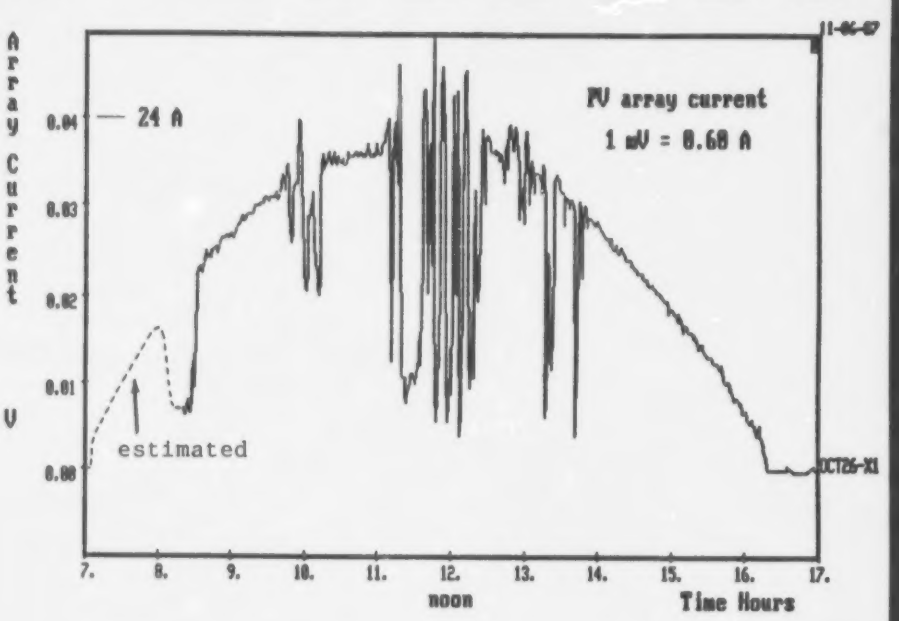

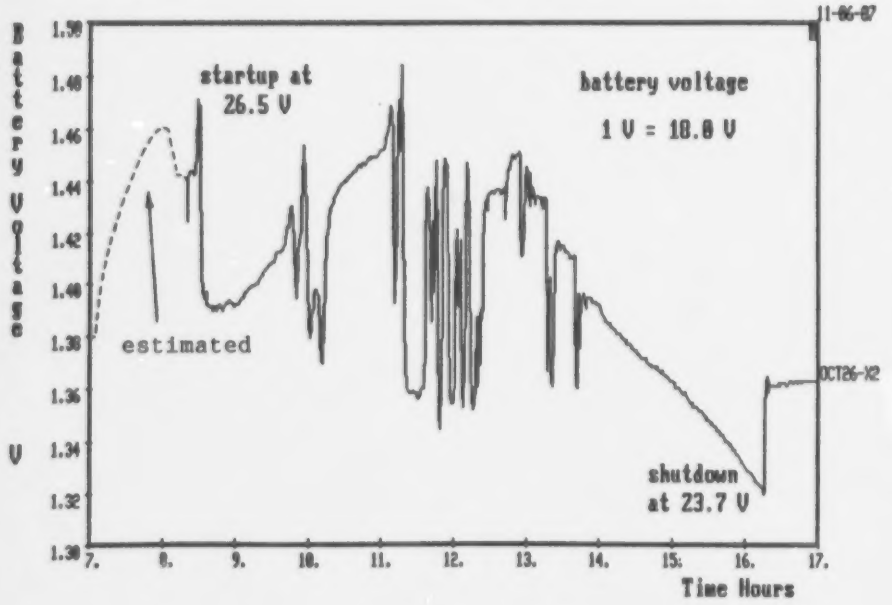

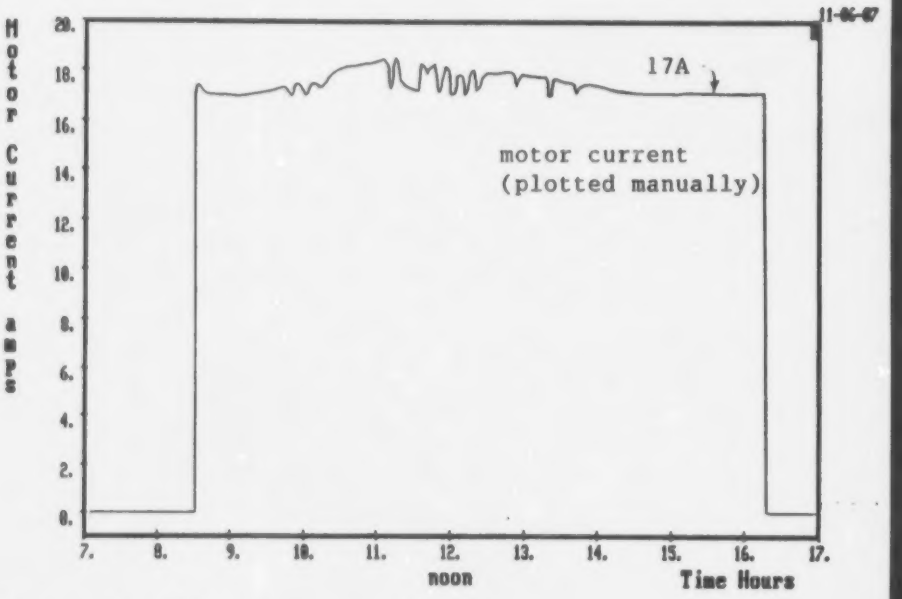

Figure 19. Prototype PV/RO system operating data for October 26, 1987.

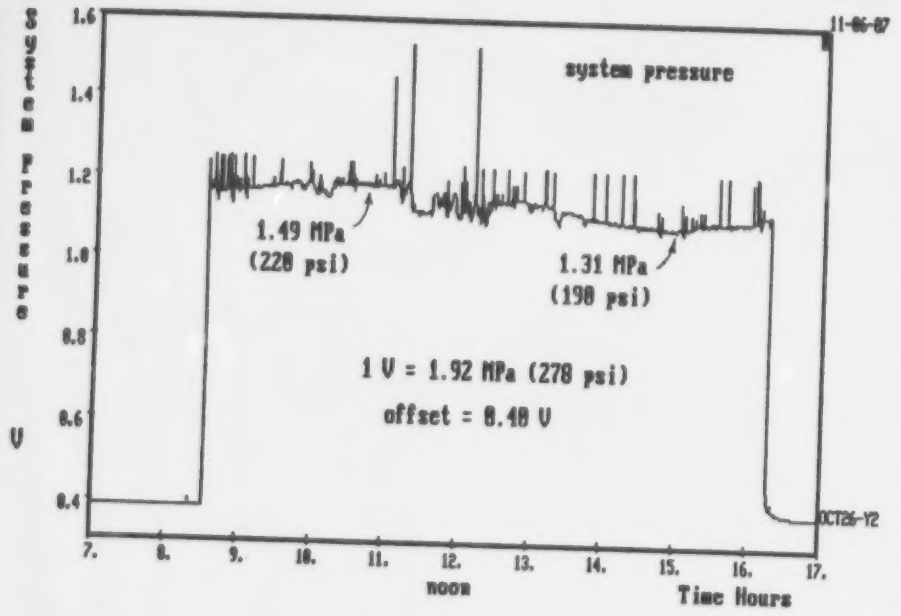

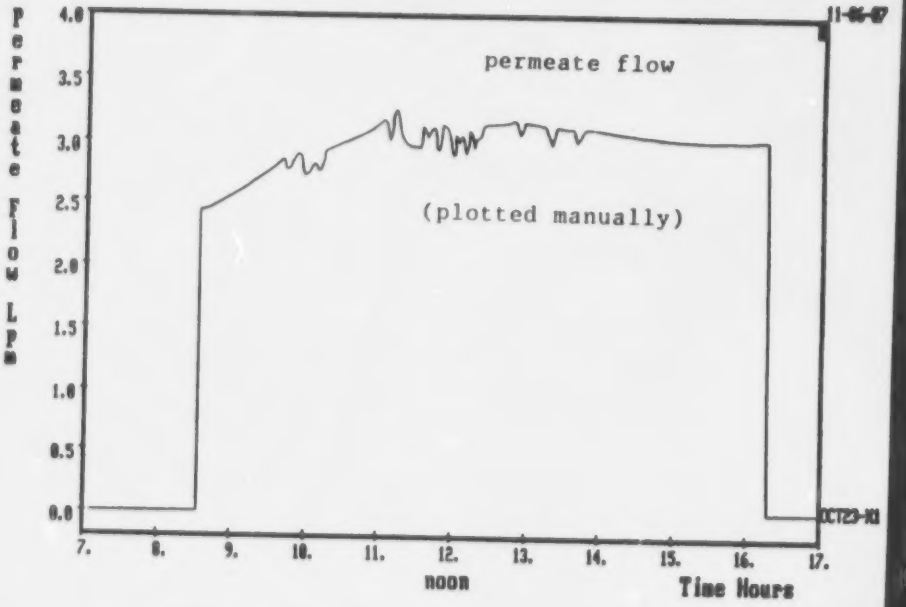

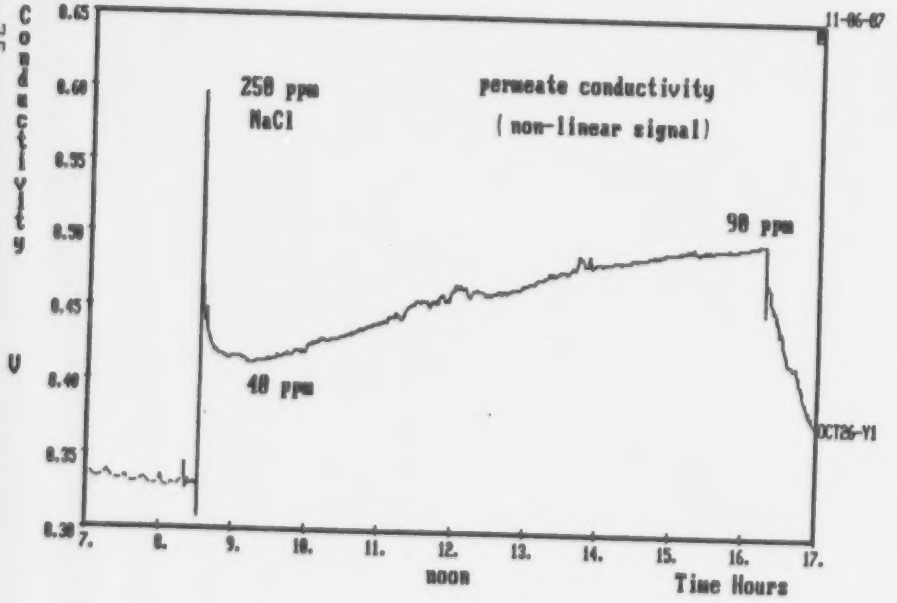

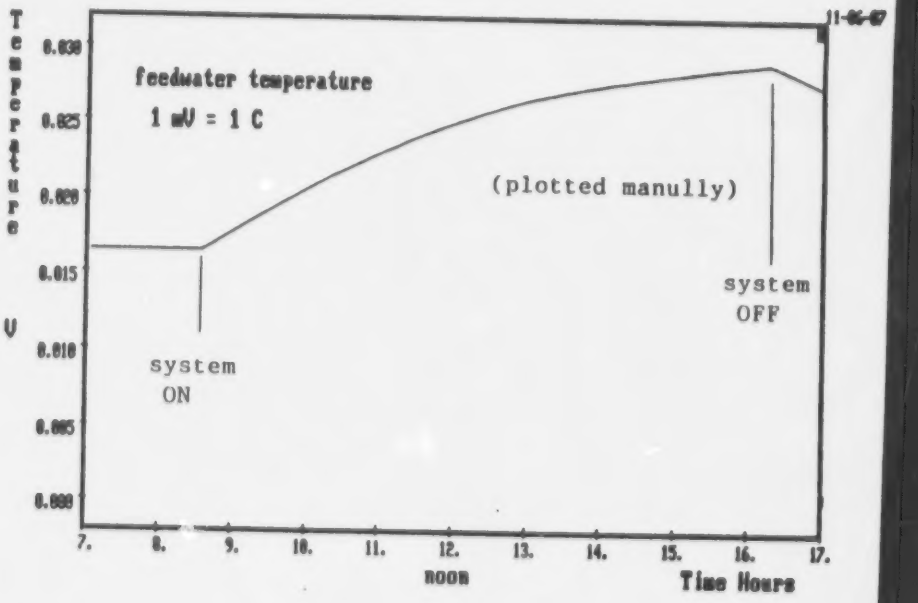

Figure 19. (continued) October 26, 1987 operating data.

TABLE I

RO SYSTEM SPECIFICATIONS

FEEDWATER QUALITY:	- approx. 3500 ppm NaCl - low solids, organics - low hardness - flow approx. 2 usgpm. (7.5 lpm)
PRODUCT WATER:	- less than 300 ppm NaCl - approx. 2.5 lpm flow rate
SYSTEM SPECS:	- 300 psi max. pressure (200 psi typical) - main pump power approx. 1/2 HP - 24 VDC supply voltage (nominal) - operating current: approx. 22 Amps
PV ARRAY:	- 750 Watts, 24 modules (2 series) - enough to operate system approx. 6 hours per day

TABLE II

COMPARISON BETWEEN TWO TYPES OF POWER CONDITIONING FOR RO SYSTEMS

CONSIDERATION	BATTERY SYSTEM	MPT SYSTEM
- ease of design	- simple (single operating point)	- difficult (all parameters interdependent and variable)
- controls	- simple: on/off	- complex: feedback
- flexibility of design	- adapts for a range of applications	- redesign for each application
- efficiency	- effective energy charging efficiency approx. 90% - no lost energy	- average MPT efficiency approx. 90% - subthreshold energy lost
- cost of power conditioning	- regulator + battery + controls approx. $800	- maximum power tracker + controls approx. $1200
- reliability	- failsafe	- suspect
- weight of power conditioning	- approx. 100 kg.	- approx. 5 kg.
- backup storage (cloudy days)	- reserve battery capacity more than one day	- none, store product water
- expected life of power conditioning	- approx. 5 years	- 10 years or more (?)
- product water per day *	- approx. 1340 l/day	- approx. 1118 l/day

* Same membranes, pumps, array used in both systems. 750 Wp array, 18 MJ/m^2/day insolation.

Table III. Test results for Hypro 5320 BHR piston pump.

Vm (V)	Im (A)	Pe (W)	speed (rpm)	η m (%)	pressure (psi)	pressure (MPa)	flow (Lpm) total	flow (Lpm) perm.	Phyd (W)	η w-w (%)	p (%)	Fr (%)
24.1	7.55	182	1971	72.0	25	0.17	9.14	0.40	26.3	14.4	20.0	4.4
24.0	8.55	206	1950	75.0	50	0.34	8.7	0.89	50.2	24.4	32.5	10.2
23.7	10.6	252	1901	78.3	100	0.69	8.1	1.70	93.0	37.0	47.2	21.0
23.7	11.1	263	1892	78.8	105	0.72	8.09	1.83	97.7	37.1	47.1	22.6
23.5	13.0	308	1851	79.5	150	1.03	7.11	2.67	123	39.9	50.2	37.5
23.4	13.5	316	1835	79.6	150	1.03	6.89	2.61	119	37.6	47.3	37.9
23.1	16.2	374	1776	79.7	215	1.48	6.47	3.55	160	42.8	53.7	54.9
23.0	18.0	414	1743	79.5	230	1.59	6.8	3.80	180	43.5	54.7	55.8

Table IV. Test results for the Procon 2502 rotary pump.

Vm (V)	Im (A)	Pe (W)	speed (rpm)	η m (%)	pressure (psi)	pressure (MPa)	flow (Lpm) total	flow (Lpm) perm.	Phyd (W)	η w-w (%)	p (%)	Fr (%)
24.1	4.26	103	1999	~55	~19	0.13	8.97	0.23	19.6	~19	~35	2.6
24.0	4.72	113	1985	~58	25	0.18	8.87	0.38	26.0	23.0	39.7	4.3
24.0	6.26	150	1976	67.5	50	0.34	8.60	0.85	49.5	33.0	48.8	9.8
24.0	7.90	190	1959	73.3	75	0.52	8.50	1.30	73.4	38.6	52.7	15.3
24.0	9.91	237	1929	77.5	100	0.69	8.23	1.76	94.7	40.0	51.6	21.4
24.0	11.9	285	1909	79.2	125	0.86	8.10	2.26	116	40.7	51.4	27.9
23.8	14.1	334	1865	79.8	150	1.03	7.87	2.74	136	40.6	50.9	34.8
23.4	16.6	388	1795	79.8	175	1.20	7.46	3.16	150	38.6	48.4	42.4
22.9	19.9	456	1710	79.2	205	1.41	7.02	3.75	165	36.3	45.8	53.4
22.1	24.8	548	1583	77.6	247	1.70	6.39	4.57	182	33.1	42.7	71.5

Table V. Sample of operating data and derived performance parameters for the prototype PV/RO system in automatic operation on Oct. 21, 1987.

time (EST)	Vb (V)	Im (A)	Tm (°C)	Tf (°C)	Ps (MPa)	Qp (Lpm)	Qb (Lpm)	η_{ww} (%)	Fr (%)	Ep (kJ/L)	Cp (ppm)	R (%)
7:39	25.04	0	~16	16	0	0	0	-	system off		-	0
11:24	~26.5	-	16	16	-	-	automatic system startup				-	0
12:02	25.00	16.4	38	18	1.44	2.54	5.08	44.7	33.3	9.69	42	98.6
12:31	24.56	16.4	49	20	1.41	2.65	5.17	45.8	33.9	9.10	40	98.7
13:00	25.24	17.1	54.5	21	1.46	2.78	5.36	45.8	34.2	9.32	42	98.6
13:34	24.37	16.5	59	22	1.39	2.80	5.22	46.1	34.9	8.62	44	98.5
14:04	24.90	16.8	60	23	1.41	2.91	5.26	46.0	35.6	8.63	45	98.5
14:44	24.15	16.2	62	24	1.34	2.80	5.06	44.8	35.6	8.38	48	98.4
15:09	23.97	16.0	62	24	1.31	2.74	5.04	44.3	35.2	8.40	50	98.3
15:35	24.08	16.0	62	24.5	1.31	2.78	5.04	44.3	35.5	8.32	51	98.3
16:12	23.84	15.8	62	25	1.30	2.75	4.88	43.8	36.0	8.22	52	98.3
16:20	23.76	-	62	25	~1.29	-	automatic system shutdown				-	0

Vb = battery voltage, Im = motor current, Tm = motor temperature, Tf = feedwater temperature, Ps = system pressure, Qp = permeate flow, Qb = brine flow, η_{ww} = wire-to-water efficiency, Fr = recovery fraction, Ep = specific energy of permeate, Cp = permeate salt concentration, R = salt rejection.

Table VI. Summary of performance of prototype PV/RO system during eleven day operating trial in October, 1987.

Oct. 1987 date	total sunlight (MJ/m^2)	array output (AH)	Tf range (°C)	total operating hours	total load (AH)	permeate volume (L)	average Ep (kJ/L)	net output ($L/MJ/m^2$)	notes
16	11.3	71.0	19-29	6.49	114.5	1234	8.14	N/A	manual start
17,18	system off and charging over weekend, no data recorded								
19	~4.7[1]	24.0	18-24	2.49	43.3	436	8.61	N/A	manual start
20	2.2	6.6	-	0	0	0	-		system off
21	~8.8[1]	52.4	16-25	4.92	80.7	809	8.85	73.5	
22	14.9	103.1	18-28	6.13	107.0	1086	8.84	72.9	
23	1.5	4.4	-	0	0	0	-		system off
24	4.1	21.2	18-21	1.30	23.0	215	9.26	38.0	
25	3.0	12.8	-	0	0	0	-		system off
26	20.1	128.4	17-29	7.74	134.6	1350	8.97	58.5	
27	9.4	56.0	~19-27[2]	3.73	59.5	599	8.68	63.7	
28	4.2	20.7	~19-22[2]	1.09	19.4	186	9.37	44.3	
Oct. 20-28	7.58	45.1	~24	2.73	47.1	472	8.90	62.2	average values

Tf = feedwater temperature, Ep = specific energy of permeate.
1 - logged irradiance data erroneous - value estimated from array current.
2 - no data recorded manually - values estimated.